BIOCHEMISTRY
including biophysical chemistry & molecular biology

Article

pubs.acs.org/biochemistry

The Q_y Absorption Spectrum of the Light-Harvesting Complex II As Determined by Structure-Based Analysis of Chlorophyll Macrocycle Deformations

Giuseppe Zucchelli,* Stefano Santabarbara, and Robert C. Jennings

CNR-Istituto di Biofisica, Sezione di Milano and Dipartimento di Biologia, Università degli Studi di Milano, via Giovanni Celoria 26, 20133 Milano Italy

Supporting Information

ABSTRACT: The absorption spectrum of the main antenna complex of photosystem II, LHCII, has been modeled using, as starting points, the chlorophyll (chl) atomic coordinates as obtained by the LHCII crystal analysis [Liu, Z., Yan, H., Wang, K., Kuang, T., Zhang, J., Gui, L., An, X., and Chang, W. (2004) *Nature 428*, 287−292] of three different trimers. The chl site Q_y transition energies have been obtained in terms of the chl macrocycle deformations influencing the energy level of the chl frontier orbitals. Using these chl site transition energy values and the entire set of interaction energies, calculated in the ideal dipole approximation, the complete Hamiltonians for the three LHCII trimers have been written and the full set of 42 eigenstates of each LHCII trimer have been calculated. With the 42 transition energies and transition dipole strengths, either unperturbed or associated to the eigenstates, the LHCII Q_y absorption spectrum has been calculated using a chl absorption band shape. These calculations have been performed both *in vacuo* and in the presence of a medium. Despite the number of approximations, a good correlation with the measured absorption spectrum of a LHCII preparation is obtained. This analysis shows that, although a substantial *C*3 symmetry of the LHCII trimer in terms of both chl−chl distances and interaction energies is present, a marked variation among monomer subsets of site transition energies is estimated. This leads to a *C*3 symmetry breaking in the unperturbed chl site transition energies set and, consequently, in the trimer eigenstates. It is also concluded that interactions among chlorophylls do not significantly modify the light absorption role of LHCII in plant leaves.

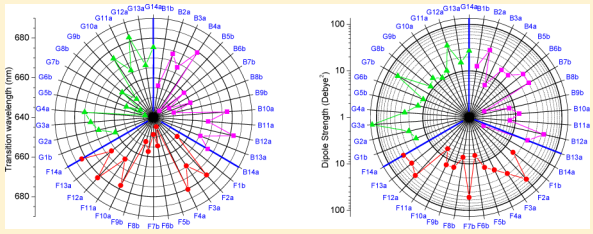

Chlorophyll (chl) molecules are bound to proteins in a number of chl−protein complexes that compose photosystems of plants[1−5] and are responsible for the characteristic Q_y absorption band of these complexes. It has also been established that the spectral characteristics of protein-bound chl molecules are modulated by interaction with their environment,[6−11] giving rise to spectroscopically different chl forms or eigenstates[11−18] having different absorption transition energies. It is also evident from the X-ray structure analysis of the chl−protein complexes crystallized up to now that a number of qualitatively different ligand−protein contacts as well as contact heterogeneity are present. Analysis of chl ring deformations,[19] presumably induced by chl−protein interactions, using the chl atomic coordinates obtained by LHCII crystal model analysis[20] suggested a correlation between chl macrocycle deformation and the modulation of the Q_y electronic transition energies. On this basis, and with respect to the planar macrocycle conformation, the range of chla Q_y absorption transitions was estimated to be about 17 nm, close to the experimental data.[19] This suggests that the uncertainty in the modeled atomic coordinates, although undoubtedly present, seems not to have a significant impact on the results. This transition energy modulation has been suggested as one of the possible sources of the chl spectral form generation.[19] This structurally induced spreading of chl energy transitions and the mutual interactions present in the chromophore array broaden the Q_y absorption band of chl−protein complexes with respect to chl absorption band in solvent (e.g., diethyl ether).[12,13,21−23] Moreover, the spread of transitions and their band shape characteristics determine a high degree of spectral congestion. Conventional absorption and fluorescence spectroscopies are unable to directly access the spectral characteristics of the chl spectral forms. The presence of a complex chl vibronic structure,[24−37] the relatively strong interactions with low frequencies protein phonons, and the presence of an intrinsic transition energy inhomogeneous broadening limit the low-temperature absorption (or fluorescence) sharpening. This prevents a direct identification of all the various energy levels characteristic of the chromophore array of chl−protein complexes. Moreover, interaction among chromophores in the array can determine changes in the distribution pattern of transition energies, giving rise to eigenstates that are, in principle, delocalized over a number of chromophores and with the transition dipole strengths being redistributed among them. This final picture is a function of both chromophore spatial organization and unperturbed chl site energy transitions, that is, those transitions

Received: November 7, 2011
Revised: March 13, 2012
Published: March 14, 2012

characteristic of chl sites in the absence of interactions among them. To disentangle the different energy transitions composing the chl−protein absorption spectrum, a number of experimental (see, e.g., refs 14, 21, 22, and 38−52) as well as numerical approaches[53−57] have been used. Site-directed mutagenesis has been used to modify major chl−protein contacts and, then, to selectively eliminate a single-site chl from the array.[9,29,47,58−60] This approach can provide the chl site transitions in the absence of substantial eigenstate delocalization and in the hypothesis of a limited perturbation of the modified protein structure caused by the mutagenesis. In the presence of delocalization the induced perturbation can modify a number of eigenstates and their transition dipole strength reorganization, preventing a straightforward interpretation of the outcome. The application of two-dimensional infrared spectroscopy,[61−64] extended to the visible range, seems to be a promising approach to directly unravel the complexity of the Q_y absorption in chl−protein complexes as well as the transfer dynamics among chlorophylls.[56,65,66] However, information concerning the site transition energies are not directly accessible from the experimental data and can only be extracted from simulation approaches, in which these data are treated as minimizable input parameters. Whereas X-ray crystal model analysis gives information on the spatial arrangement of chromophores, their mutual orientation, and distances, allowing interaction energy estimation,[20,54] information about the site-specific chromophore transition energy is lacking. This information is essential to understanding the detailed optical properties of the chl−protein complex as well as energy transfer in chromophore antenna reaction center arrays.

We focus our attention on LHCII, the major light-harvesting antenna of PSII. This chl−protein complex is known to be composed of three monomers arranged according to *C*3 symmetry.[67] The recent crystal X-ray data analysis[20] of spinach LHCII, while substantially confirming previous structural information on LHCII obtained from single-particle analysis of microcrystalline arrays,[67] allowed the identification of the chl species in each chl site. Fourteen chlorophylls are identified per monomer, eight chla and six chlb, which appear to be arranged in two layers, the lumenal and the stromal layers, with respect to membrane orientation.[20] Interestingly, an important aspect of the structural study of Liu et al.[20] is the presence of 10 distinguishable monomeric LHCII complexes, 9 of which are organized into three trimers. A total of 80 chla and 60 chlb molecules are then described in terms of their atomic coordinates.

These X-ray data have been used to define the model Hamiltonian in terms of chl site energies and the associated set of interactions, which were then employed in the numerical fitting of LHCII optical spectra[53] and 2D electronic spectra.[56] On the basis of trimer symmetry consideration 14 different site energies were taken into account, and the unperturbed chl site transition energies were indirectly obtained by a fit procedure of the LHCII optical spectra. A combined quantum chemical/electrostatic method has been recently applied to LHCII[57] using the crystal structure data,[20,68] and 14 eigenstate energies as well as chl site energies have been directly modeled.

In this paper we use a different approach to directly estimate the chl Q_y site transition energies of LHCII in terms of the analysis of the chl ring deformation[19] using the X-ray crystal data.[20] It has been shown that it is possible to connect the lowest energy normal modes of deformations to displacements of the energy of the frontier chl orbitals that control the Q_y absorption transition. This analysis has been applied to the three different LHCII trimer structure models obtained by Liu et al.,[20] allowing also the comparison of different single LHCII complex realizations.

The main aim of this paper is to understand if it is possible to describe the LHCII Q_y absorption band in terms of the chl macrocycle deformation imposed by interaction with the protein. The results confirm this.

To summarize, in the present study the following points are addressed: (1) Direct calculation is made of all the intrinsic chl transition energies in terms of the chl structures as obtained from the three LHCII trimer crystal data.[20] These Q_y transition energies are calculated in the absence of other sources of energy modulation other than chl deformations. This is done both considering *in vacuo* condition and then in the presence of a medium that takes into account the nonspecific solvatochromic effect as a source of transition energy shift. Refractive index heterogeneity, characteristic of the chl surroundings, is discussed. (2) The interaction energies for the full set of 42 chlorophylls of each of the three LHCII trimers are calculated in the ideal dipole approximation. This is discussed both for the *in vacuo* case and in the presence of the intervening medium that attenuates the interaction energies as a function of chl−chl distance. (3) Analysis of the complete set of 42 eigenstates of each of the three LHCII trimers gives their transition energies (eigenvalues), chl site contributions to the eigenstates, redistributed transition dipole strengths, and an estimation of eigenstate delocalization in terms of the inverse participation ratio.

The *in vacuo* condition is useful in that it provides an understanding of the impact of the chl array geometry and characteristic macrocycle distortions on the absorption transition characteristics. The eigenstate properties are used to directly calculate the RT LHCII Q_y absorption spectrum. It is shown that, despite the approximations used, a quite good correspondence between calculated and measured absorption spectra is obtained. The role of chl−chl interactions in determining the light absorption role of LHCII in plant leaves is also discussed.

THEORY

To obtain a direct evaluation of the LHCII eigenstates that define its optical properties, knowledge of the set of both the intrinsic chl transition energies, that is the chl site energies in the absence of mutual interactions, as well as the full set of interaction energies among all the chlorophylls composing the chromophore array is necessary. Both of these elements will be directly evaluated using the structure data based on the X-ray diffraction model of the LHCII complex crystallized by Liu et al.[20]

Structural Unperturbed Transition Energies. Structure-based calculations of the intrinsic chl transition energies have been performed as previously described,[19] using the chl structural data[20] obtained for the three crystallized LHCII trimers (Protein Data Bank 1RWT) and in terms of the Normal Coordinate Structural Decomposition method[69−71] to evaluate the chl macrocycle deformations. Some of these deformations, in fact, modify the energy of the chl frontier orbitals involved in the Q_y electronic transition.[19] These calculated transition energies, modulated by chl interactions with the protein backbone only, are here defined as unperturbed. The protein sequences of the nine chains composing the three LHCII trimers are identical (PDB Protein Comparison Tool).

Nevertheless, analysis of the interatomic contacts ligand−protein (http://ligin.weizmann.ac.il/cgi-bib/lpccsu[72]) performed on the LHCII ligands of the different protein chains (not shown) suggests the presence of conformational variability among the nine monomers composing the three trimers. It is hypothesized here that the three LHCII trimers analyzed represent independent conformational protein−ligand subsets,[73] frozen during crystallization, and their structure provides an idea of the solubilized LHCII conformational variability in detergent/solution mixtures.

Chl ring deformation is not the sole factor that concurs in establishing the chl absorption transition energy in chl−protein complexes. Other factors that need to be considered are, for example, interactions with the microenvironment (see, e.g., ref 10) as well as among chlorophylls.

Modulation of Chlorophyll Transition Energies by the Environment. The presence of the surrounding medium acts to shift chl electronic site transition energies via the solvatochromic effect.[74−76] This effect is associated with reorganization of the surrounding "solvent" and depends on the refractive index of the medium around the chromophore. The solvatochromic effect plays a major role in solution[75,76] and, presumably, is also relevant in the presence of a nonisotropic medium such as is the protein host. The solvatochromic effect was analyzed for chla[75,76] in a number of different solvents. The nonspecific solvent effect on the chl wavelength (nm) absorption transition *in vacuo*, λ_0, can be described by a parametrized semiempirical equation[75]

$$\lambda = \lambda_0 + 38.3\left[\frac{n^2-1}{2n^2+1} + 0.73\frac{2n^2+1}{n^2+2}\left(\frac{n^2-1}{n^2+2} + 0.058\left(\frac{D-1}{D+2} - \frac{n^2-1}{n^2+2}\right)\right)\right] \quad (1)$$

where n is the refractive index and D the dielectric constant of the surrounding solvent. This relationship will be used here to evaluate the impact of the solvatochromic effect on the calculated, unperturbed, chl site Q_y wavelength transitions,[19] identified as λ_0, after appropriate choices of the values for n and D.

Whereas both the refractive index and the dielectric constant are readily measurable in bulk isotropic solvents, their values for a protein environment are not able to be determined in a straightforward way. Refractive index values in the range of 1.36−1.55 have been proposed for adsorbed protein layers as a function of the protein size.[77] The lower estimated value is close to the refractive index of water (~1.33 at room temperature). Refractive indices in the range of n = 1.51−1.65 were instead estimated using different chl−protein complexes,[78−81] values that sit on the upper bound of the range determined by Voros.[77] It is interesting to note that an even larger value (n = 1.86) has been proposed for the violaxantin environment in LHCII,[80] suggesting a marked refractive index heterogeneity in LHCII. Values for the dielectric constant D in the range of 4.6−6.8 have been estimated for protein,[82−84] although, sometimes, dielectric constants up to 20 are utilized.[84] However, D has only a small effect on the red shift of the electronic transition as described by eq 1.[19]

Although it is usual to adopt single values of n and D for all of the chl environments in chl−protein complexes, chl molecules seem to have different surroundings in LHCII structure.[20] In particular, some chlorophylls are facing outside the protein backbone, presumably in partial interaction with the bulk solvent, whereas others seem well buried inside the protein backbone. To have an idea of these different environments, the chl solvent-accessible surfaces[72] have been calculated using the analysis of ligand−protein contacts at the LPC/CSU server (http://ligin.weizmann.ac.il/lpccsu). These surface values are regarded as a first approximation of the solvation free energy.[85] The presence of the phytolic chain does not interfere with the chl first solvation cell[86] and has a limited effect on the chl transition energy.[86,87] The contribution of the phytolic chain to the solvent-accessible surfaces is then neglected, and only the chl macrocycle contribution is taken into account. The results are shown in Figure 1, where at least two different

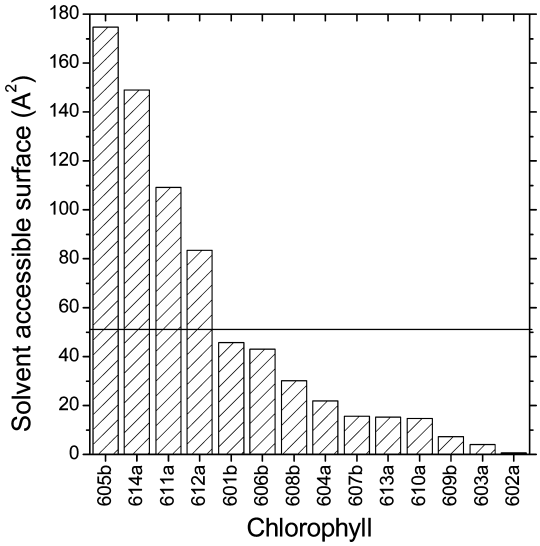

Figure 1. Chlorophyll solvent-accessible surface. The data are the mean of three different evaluations for each chl in different LHCII monomers obtained using the analysis of ligand−protein contacts at the LPC/CSU server (http://ligin.weizmann.ac.il/lpccsu). See Methods for further details. Chlorophylls are numbered according to the guidelines of Liu et al.[20] with a and b indicating the chl type. The horizontal line marks the total mean surface (51 Å²).

chromophore populations are recognized. Four chlorophylls have solvent-accessible surfaces that are well above the total mean value (51 Å²). These are chlb 605 (chlorophylls numbered according to ref 20) and three chla, 611, 612, and 614, whereas the others have lower values. We then consider, as a first approximation, two different chl surroundings characterized by different refractive indices, lower for the environment of the four chlorophylls with the greatest accessible surfaces. For these last chlorophylls we chose the lowest refractive index value n = 1.36 proposed for adsorbed protein layers,[77] whereas refractive indices in the range of n = 1.51−1.65, as estimated for chl−protein complexes,[79−81] are used for protein-buried chlorophylls. The dielectric constant D = 5 is used in all of the solvatochromic shift calculations. No other sources of absorption transition energy shift have been considered.

Interaction Energies. The coupling strengths among chlorophylls in chl−protein complexes have been often obtained in the ideal dipole approximation (see, e.g., ref 10), although to overcome the limits inherent in this approach, different quantum chemical calculations, using various methods,

dx.doi.org/10.1021/bi201677q | *Biochemistry* 2012, 51, 2717−2736

have been recently performed on LHCII structure model data.[54,57,88] In particular, Frahmcke and Walla[54] compared the calculated Coulombic couplings among LHCII chlorophylls using an *ab initio* approach with the LHCII crystal data [20] to the couplings obtained in the ideal dipole approximation. They found marked deviations between the two approaches for Q_y-Q_x and Q_x-Q_x chl interactions below 25 Å mutual distances. However, the two approaches give similar results for Q_y-Q_y interactions[54] also at short chl distances. A similar conclusion concerning Q_y-Q_y chl interactions has been recently obtained for LHCII using a different numerical method.[57] As we consider only Q_y interactions, the ideal dipole approximation is then considered to be a suitable approximation, and the interaction energy strength V_{ij} between the ith and jth chromophores of the trimer array is

$$V_{ij} = \alpha\kappa_{ij}\frac{\mu_i\mu_j}{R_{ij}^3} \tag{2}$$

where R_{ij} is the distance between the ith and jth chromophores and $\overline{R}_{ij}$ is its versor (unit vector); μ_i is the ith transition dipole moment, and $\overline{\mu}_i$ is the versor, oriented along the ith dipole; $\kappa_{ij} = \overline{\mu}_i\cdot\overline{\mu}_j - 3(\overline{\mu}_i\cdot\overline{R}_{ij})(\overline{\mu}_j\cdot\overline{R}_{ij})$ is the orientation factor defined in terms of distance versors and transition dipole moment versors. The remaining parameter is the attenuation coefficient, α, that accounts for the presence of the medium. *In vacuo* $\alpha = 1$. When the transition dipole strength is expressed in Debye^2 and the distance in nm and a multiplicative constant of 5.034 is considered, the interaction energy strength is given in cm^{-1}.

The distances R_{ij} between the ith and jth chl molecules in a trimer are here defined in terms of the "centers" of the tetrapyrrole rings, calculated as the mean values (x, y, z) of the four chl nitrogen coordinates obtained by LHCII crystal analysis.[20]

The electronic transition dipole moment vector is taken along the axis through the NB−ND chl nitrogen atoms (y direction), oriented toward ND, and has been estimated for each chl using the crystal nitrogen coordinates.[20] This is an approximation as the molecular transition dipole direction depends on the atomic charge distribution that is, presumably, modulated by the chlorophylls' puckered configurations.[19] This modulation could be a factor in the description of the LD and CD signals, in which the geometry of the sample is directly involved.

The unperturbed transition dipole strength values μ_i^2 (Debye^2), that is, the dipole strength in the absence of interactions, are calculated using the phenomenological equation[89,90]

$$\mu^2 = 20.2 + 23.6(n - 1) \tag{3}$$

which, in the limit of the refractive index $n = 1$, predicts the chla transition dipole strength *in vacuo*.[89,90] This extrapolated value is in good agreement with vacuum values obtained using a theoretical approach.[89] The presence of the medium acts to modify the chl transition dipole strength value, but the choice of the refractive index value in eq 3 is an open problem. When the medium is represented as a bulk continuum described by the refractive index, this parameter is considered as characteristic of a portion of space of the order of the wavelength of the light interacting with the sample (see, e.g., refs 89 and 91). In this view, as the LHCII trimer has a diameter of the order of 60−75 Å, 2 orders of magnitude smaller than the wavelength of visible light, the presence of the chl−protein complex is only a slight perturbation and the refractive index used is that of the host medium (solvent picture). Then, for LHCII in solution, the refractive index of water ($n \sim 1.33$) is chosen to modulate the chl transition dipole strength value and eq 3 gives $\mu^2 \cong 28$ D^2 for chla.

The last parameter involved in the interaction energy calculation (eq 2) is the attenuation term α. As the Coulombic energy coupling induces electronic excitation energy transfer among molecules, the effect of the host medium surrounding the molecules and the choice of the attenuation factor are central topics in the excitation energy transfer analysis and modeling. These topics have, in recent times, enjoyed renewed interest (see, e.g. refs 92−94). The Förster approach, commonly used, considers the screening factor having the functional form $\alpha \equiv n^{-2}$, where n is the refractive index. Interaction energies are then reduced by a constant factor and no other dependencies are considered. Knox and van Amerongen[92] discussed the Förster attenuation, suggesting that it is the refractive index of the protein environment that must be taken into account (local picture). However, in recent studies investigating the effect of the host medium on electronic energy transfer[93,94] it has been proposed that when chromophores are close enough to exclude solvent, attenuation becomes reduced, thus introducing a screening factor distance dependency. This is summarized in a semiempirical equation[93,94]

$$\alpha = A\ e^{-\beta R} + \alpha_0 \tag{4}$$

where α_0 represents the asymptotic screening value, β the steepness of the distance dependent attenuation, and R the interchromophore distance ($R = R_{i,j}\ \forall i,j$). A is a parameter that renders $\alpha = 1$ (no attenuation) when a minimal distance between chromophores is reached and the chromophores are in the same cavity in the medium (see the Supporting Information). It is worth stressing that the parameters A, β, and α_0 all depend on the refractive index of the immediate chromophore environment, including protein and intrinsic water (see the Supporting Information). At short chromophore mutual distances, when attenuation disappears, $\alpha = 1$. At longer distances, when the full refractive index of the environment becomes effective, the maximum attenuation, $\alpha_0 < 1$, is reached. The exponential decreasing attenuation given by eq 4 induces sizable interaction energy changes in the initial decreasing phase with respect to the pure Förster attenuation approach. Both short and asymptotic distances are defined as specific properties of the object analyzed.[93,94] According to these studies, the asymptotic screening value is, roughly, midway between the Förster $1/n^2$ attenuation value and the Onsager value $3/(2n^2 + 1)$ and parameters of eq 4 have been estimated[94] considering a host medium with $n = 1.414$. Because of higher refractive index values in chl−protein complexes,[79,80] the refractive index dependence of eq 4 has been made explicit (see the Supporting Information).

To summarize, the interaction energy (eq 2) can then be written

$$V_{ij} = \left[\rho\ e^{-\left((R_{ij}-R_f)/(R_f-R_0)\right)\ln\left(\frac{1-\alpha_0(n_L)}{\rho}\right)} + \alpha_0(n_L)\right] \kappa_{ij}\frac{20.2 + 23.6(n - 1)}{R_{ij}^3}\sqrt{a_i a_j} \tag{5}$$

dx.doi.org/10.1021/bi201677q | *Biochemistry* 2012, 51, 2717−2736

where $\alpha_0(n_L) = 1/2((5n_L^2 + 1)/(n_L^2(2n_L^2 + 1)))$; $\rho = 0.0035$, R_0 is the maximal distance between chlorophylls that gives no attenuation ($\alpha = 1$), and R_f is the minimal distance between chlorophylls at which the asymptotic attenuation is reached. We have used $R_0 = 6.6$ Å and $R_f = 26$ Å (see the Supporting Information). The parameter a_i takes into account the presence of chla and chlb, with monomer chlb transition dipole strength being 0.7 that of chla (see, e.g., ref 95). Thus, $a_i = 1$ for chla and $a_i = 0.7$ for chlb, under the assumption that the transition dipole strength ratio between chla and chlb is independent of the refractive index. Two refractive indices are present in eq 5, the refractive index of the bulk medium, n, taken as $n = 1.33$, and the refractive index that reflects local properties, n_L. Values of n_L in the range of 1.36−1.60 have been used, from the lowest refractive index value obtained for protein films[77] to those obtained for photosynthetic chl−protein complexes.[79−81] Equation 5 gives the interaction energies due to LHCII trimer structural properties and includes their environmental modulation. We remark again that, in the absence of other information, we assume that all chla molecules in LHCII have the same unperturbed transition dipole strength as well as all chlb.

METHODS

Using the full set of Q_y-Q_y interaction energies, V_{ij}, among the 42 chlorophylls in a trimer and the 42 independent transition energies for all chl sites, evaluated in terms of chl macrocycle deformations[19] and modulated by the environment, a 42 × 42 matrix was compiled for each of the three LHCII trimers based on crystal data model analysis.[20] These matrices were numerically diagonalized (Maple 12, Maplesoft) and the full sets of 42 eigenstates calculated. The eigenstates are described by their transition energies (eigenvalues) and the normalized eigenvectors containing the weighted contribution e_i of all chlorophylls in a trimer. Normalized means that $\sum_{i=1}^{42} e_i^2 = 1$.

To measure the localization/delocalization of the different eigenstates, the so-called participation ratio (PPR)[96] has been calculated. This parameter, interpreted as a measure of the number of sites that gives a significant contribution to an eigenstate, is defined as

$$\mathrm{PPR}_k = \left(\sum_{i=1}^{N} e_{k,i}^4\right)^{-1} \tag{7}$$

where N is the number of sites (dimensionality of the vector space) and $e_{k,i}$ is the ith contribution to the eigenvector of the kth eigenstate.

Eigenstate Transition Dipole Strength. The interactions among chlorophylls redistribute the unperturbed single-site chl transition dipole strengths in the eigenstates of the chromophore array. To determine this redistribution, the transition dipole strength associated with each eigenstate has been calculated. The Q_y transition dipole strength for the kth eigenstate is defined, as usual, by

$$\mu_k^2 = \sum_{i,j}^{N} |\vec{\mu}_i||\vec{\mu}_j|(\bar{\mu}_i \cdot \bar{\mu}_j) e_{k,i} e_{k,j} \tag{8}$$

where N is the number of molecules in the array, $\vec{\mu}_i$ is the effective transition moment, $\bar{\mu}_i$ is the versor along the ith transition dipole, and $e_{k,i}$ is the ith element of the eigenvector of the kth eigenstate obtained by the diagonalization of the 42 × 42 matrix. The sum of the 42 eigenstates transition dipole strengths is equal to the sum of the 42 unperturbed chlorophyll transition dipole strengths (sum rule), an approximation that holds when the wavelength of light is greater than the interacting object,[97] as is the case for LHCII.

Absorption Spectrum Calculation. Knowledge of the 42 eigenstates, with their transition energies and associated redistributed transition dipole strengths, permits calculation of the absorption spectra for the three LHCII trimers analyzed.[20] To this end a chl band shape, located at each eigenvalue (transition energy), with area equal to the eigenstate transition dipole strength value is associated with each eigenstate. The same chl band shape has been assumed for all eigenstates, although the presence of some band shape heterogeneity has been indicated.[60] The band shape has been calculated using the vibronic pattern obtained by hole burning[24] and the associated Franck−Condon factors obtained by fitting the chla absorption spectrum measured in diethyl ether, as already described.[98] A mean low-frequency phonon mode, often found in chl−protein complexes and which has approximate values of $\nu = 20$ cm^{-1} and coupling $S = 0.8$,[24,37] contributes to the homogeneous absorption bandwidth. A normally distributed inhomogeneous contribution to the total bandwidth is also taken into account to permit comparison with the experimental LHCII absorption spectrum. The values considered are indicated in the figure captions.

It is interesting to note that in the presence of strong interaction, besides intensity redistribution among the exciton peaks, the exciton bandshapes become narrower than the band shape of the corresponding noninteracting monomer band shape. This band-narrowing effect has not been considered in the following calculations.

Chlorophyll Nomenclature. The nomenclature of Liu et al.[20] is used to identify the different chlorophylls with an added index to denote chl type (e.g., 601_b means chlb 601). Three different LHCII trimers are present in the Protein Data Bank (1RWT) indicated by letters, BFG, CHE, DIJ, that identify the monomers. The 14 chlorophylls belonging to each monomer are here specified by the letter labeling the monomer followed by chl number. As an example, B1b is chlb 601 of the B monomer of the BFG trimer, B14a is chla 614 of the same monomer. When the calculated eigenstates are considered, they are identified in terms of the major chl contribution to the relative eigenvectors (e.g., B1b is the eigenstate with eigenvector containing the major contribution due to chlb 601 of the B monomer).

RESULTS AND DISCUSSION

Interaction among chlorophylls is the driving force that causes eigenstate delocalization over the chromophore arrays, in competition with both diagonal (site energy) and off-diagonal (interaction energy) disorder that, when present, tends instead to localize the eigenstates. The final eigenstate energy transition (eigenvalues) distribution is modified by interactions and depends strongly on the unperturbed chl site energies set. Hence, knowledge of the unperturbed chl site electronic transition energy is crucial in understanding how the structure determines the final optical properties of the chl−protein complexes. Moreover, the presence of a network of interactions among chromophores, besides scattering the chl contributions among different eigenstates with new distributions of transition energies, also causes a redistribution of the chl transition dipole strength over the eigenstates that can be significant. Therefore,

dx.doi.org/10.1021/bi201677q | Biochemistry 2012, 51, 2717−2736

to gain information about the redistributed transition dipole strength, the complete interaction network needs to be considered. The calculated intrinsic unperturbed chlorophyll transition energies set is the starting point to evaluate the effect due to different perturbations that lead to the final LHCII eigenstate distribution. This eigenstate distribution will be evaluated initially in the absence of a medium (n = 1, D = 1), when no interaction energy attenuation and solvatochromic effect are present, and then when a medium is instead present. This highlights the role of chl macrocycle distortion.

Interaction Energies *in Vacuo*. To gain an idea of the intrinsic structural properties of chlorophylls in LHCII only the bare structures obtained from the crystal data[20] for the three different LHCII trimers are considered *in vacuo*. The values of the calculated interaction energies, in the ideal dipole approximation, are obtained using chla transition dipole strength μ^2 = 20.2 D^2 (eq 3), whereas the chlb transition dipole strength is taken to be 0.7 the chla value (see e.g., ref 95). No attenuation is present (Supporting Information, Figures S2, S3, and S4 for the three trimers).

The main interacting couples are those already reported.[20,53,54] Of the three highest determined interaction energies (e.g., Supporting Information, Figures S2, S3, and S4), two are between mixed chl a/b couples (603_a–609_b; 604_a–606_b). The strongest structural interaction energy is between chl 611_a and 612_a.[20,54,57] In addition, as already observed,[20] chl 609_b of one monomer interacts significantly with the facing chlb, 601_b, on the adjacent monomer in a trimer. Moreover, chl 601_b interacts with a similar value of the interaction energy also with chl 602_a on the same monomer.

Interaction energies between *C*3 symmetry related couples in a trimer are similar, and this also applies to the interaction energy distribution of the three trimers (Supporting Information, Figures S2, S3, and S4). The LHCII trimer has then, in terms of the interaction energy pattern, a substantial *C*3 symmetry and the off-diagonal disorder seems low. We emphasize this aspect as it will be shown that the site transition energies are markedly variable.

Unperturbed Site Transition Energies. An estimation of the chla and chlb intrinsic transition energies in LHCII have been recently proposed[19] in terms of the chl ring deformations obtained by chl crystal coordinates[20] and analyzed by normal-coordinate structural decomposition.[69−71] Variability of the chl macrocycle deformation pattern is present both among *C*3 site-related chlorophylls in a trimer as well as among chlorophylls in the same site of different trimers resulting from subtle structural differences among LHCII monomers. This variability is reflected to variability of the unperturbed transition energies (Figure 2). We recall that these transitions are due to LHCII structural characteristics, in the absence of chl interactions, or other contributions that lead to energy shifts (e.g., solvatochromic effect). Besides heterogeneity among trimers, the clover leaf representation of Figure 2 shows that chl site transition energies within a trimer are also not *C*3 related. These differences, of structural origin, determine a symmetry breaking in the LHCII trimers organization, indicating the presence of diagonal disorder in LHCII trimers.

LHCII Eigenstates *in Vacuo*. The characteristics of the 42 eigenstates (see Methods) calculated from the unperturbed electronic site energies (Figure 2) and the entire set of chl interaction energies (partially shown in Figures S2, S3, and S4 of the Supporting Information), are shown in Figure 3 for the

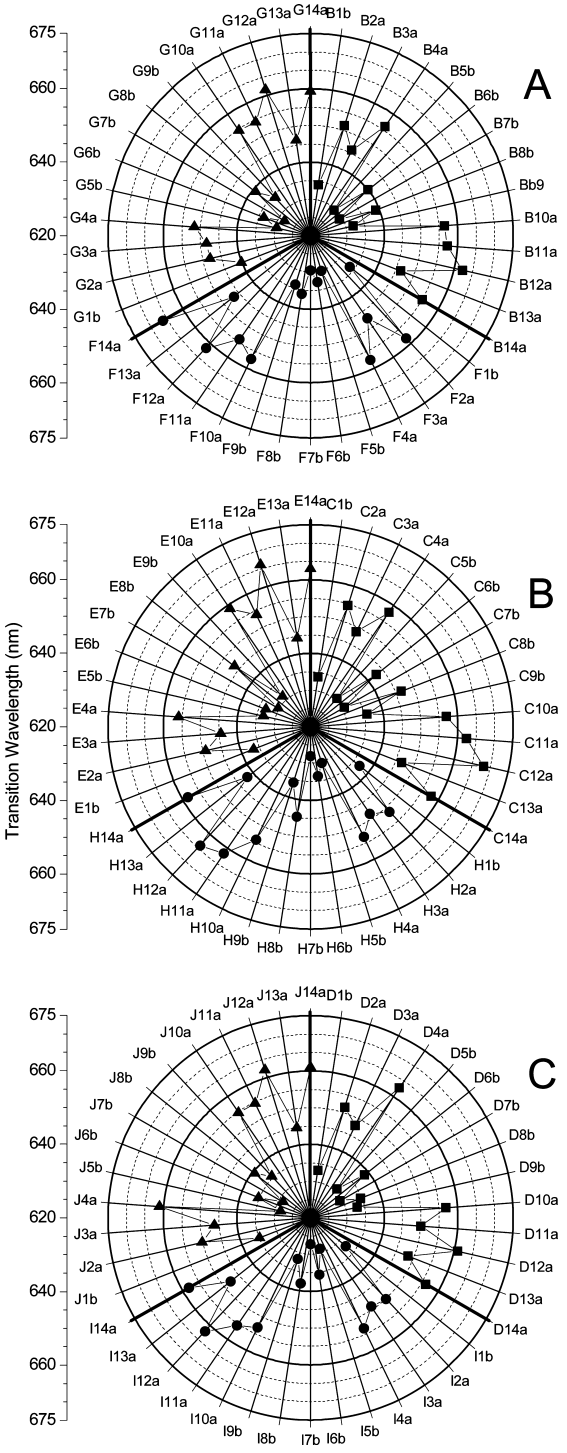

Figure 2. Structural transition wavelengths for chlorophylls in the three LHCII trimers: (A) wavelength transitions for the BFG trimer (nomenclature according to that of Liu et al.[20]); (B) wavelength transitions for the CHE trimer; (C) wavelength transitions for the DIJ trimer. Symbols represent chlorophylls belonging to the different monomer. The wavelengths have been calculated according to the method of Zucchelli et al.[19] (see also Methods) using chl crystallographic coordinates.[20] The different monomers of LHCII trimer are marked by heavy radii. Each ray represents a chl site (e.g., B1b means chlb 601 of the B monomer of the BFG trimer, B2a means chla 602 of the same monomer, and so on), and symbols on each ray mark the transition wavelength associated with that site.

dx.doi.org/10.1021/bi201677q | *Biochemistry* 2012, 51, 2717−2736

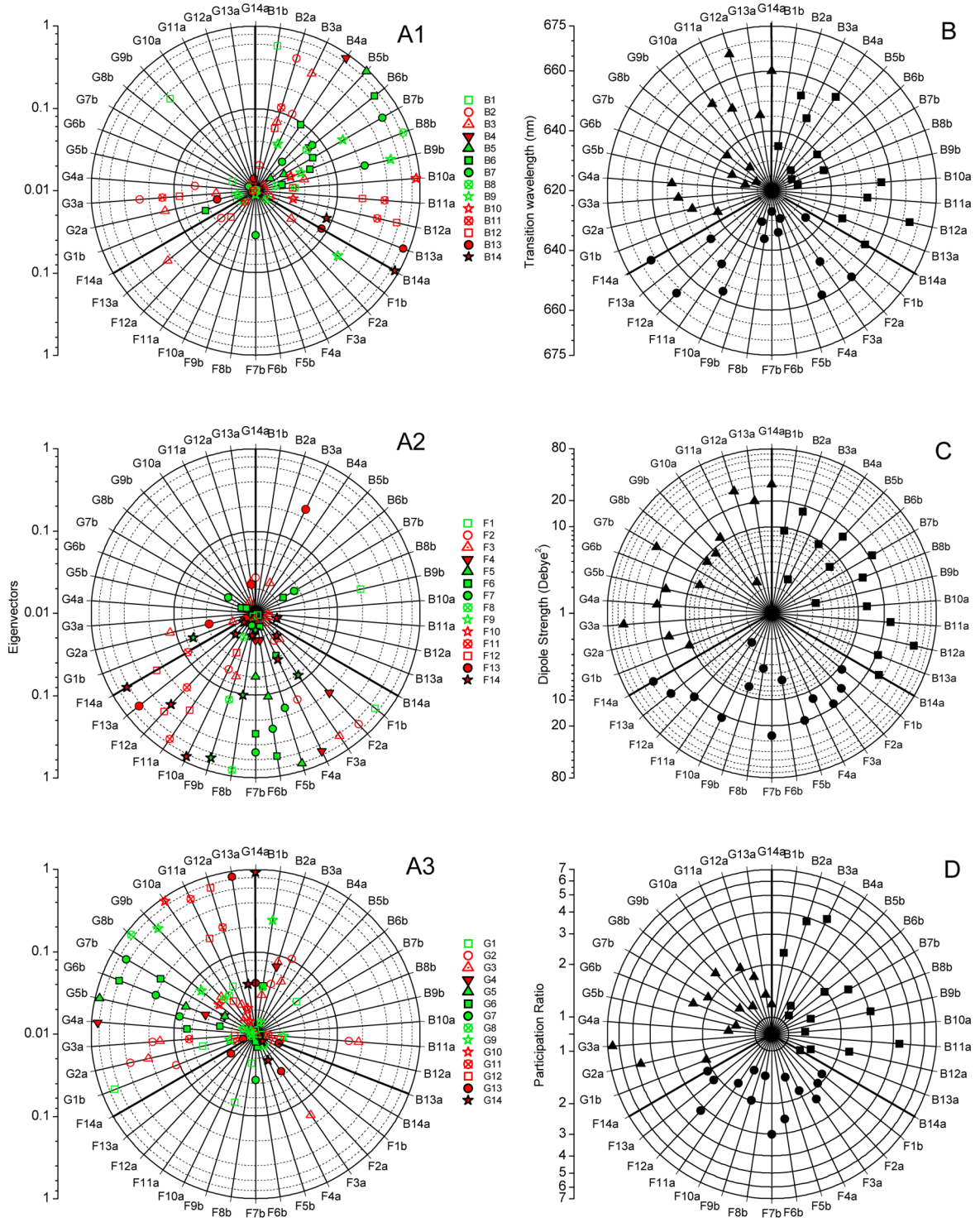

Figure 3. Eigenstate properties for the LHCII BFG trimer *in vacuo*. Panels A1, A2, and A3 show the squared contribution of all the chlorophylls of the B, F, and G monomers, respectively, to the 42 eigenstates identified by the 42 radii and, on each radius, by the dominant chl contribution. The scale is logarithmic. Heavy radii mark the boundaries of monomers and polar representation highlights C3 symmetry. (Open symbols) chlorophylls of the stromal layer; (solid symbols) chlorophylls of the lumenal layer; (red symbols) chla; (green symbols) chlb. As an example, in panel A1 the radius B1b indicates the eigenstate dominated by the contribution of chlb 601 of the B monomer. Looking at the same marked radius in the three panels, the complete chl contributions to the given eigenstate can be obtained. For example, the B1b eigenstate contains, other than the dominant (60%) contribution by chl B1b, also 2% of B2a (red open circles) (panel A1), 25% of G9b, and 3−4% of G3a, G6b, and G8b (panel A3). On the other hand, the contribution of each chl to the eigenstates can be recognized by looking at the same symbol in each panel. As an example (Figure 4A1, B monomer), chl B1b, besides contributing maximally (60%) to the B1b eigenstate, contributes also to the G9b eigenstate (33%) and to the G6b eigenstate (≈2%). The remaining 5% is scattered among other eigenstates with contributions ≤1% (not shown). Panel B shows the transition wavelengths (eigenvalues) associated with the 42 eigenstates specified by the dominant chl contribution. Panel C shows the eigenstate-associated dipole strength as redistributed by chl−chl interactions in logarithmic scale. The initially unperturbed chla dipole strength is dps = 20.2 D^2. Panel D

dx.doi.org/10.1021/bi201677q | *Biochemistry* 2012, 51, 2717−2736

Figure 3. continued

shows the inverse participation ratio (see the text and the Supporting Information) associated with each eigenstate in logarithmic scale. This parameter gives a measure of the delocalization of the eigenstate in terms of chl equivalent.

BFG trimer (see also Figures S5 and S6 of the Supporting Information for CHE and DIJ trimers, respectively).

Comparison of each unperturbed chl transition (Figure 2) with the eigenvalue of the eigenstate dominated by the same chl contribution (Figure 3 and Figure S7 of the Supporting Information) shows that the majority of eigenvalues are shifted by $< \pm 2$ nm by chl−chl interactions. This is due to the presence of a great number of low-energy interactions and to large intrinsic site energy gaps. It is interesting to note that interaction energies obtained in the ideal dipole approximation are similar to or greater than those obtained by other approaches.[54] Hence, even when different approaches to calculate the interations are considered, this would not lead to a larger shift of the eigenstate transition energies which, in essence, are then determined predominantly by the unperturbed site energies.

The chl 611_a and 612_a dominated eigenstates undergo the greatest energy transition splitting (Figure S7 of theSupporting Information), as is expected in terms of the interaction energy values and unperturbed transition energy differences, with the chl 612_a dominated eigenstate having the greatest red shift (5.4 ± 0.7 nm, BFG trimer) and the chl 611_a dominated eigenstate the greatest blue shift (4.4 ± 0.7 nm, BFG trimer). The chl 612_a dominated eigenstate is the redmost (Figure 3B and Figures S5 and S6 of theSupporting Information), due also to the fact that, in terms of macrocycle deformations, chl 612_a is, on average, the redmost unperturbed chl (Figure 2).[19] The other two major interacting couples are mixed chla−chlb (603_a−609_b; 604_a−606_b), and their unperturbed site transition energy differences lead to a more reduced splitting between related eigenstates (Figures 2 and 3 and Figure S7 of theSupporting Information). Nevertheless, eigenstates dominated by chl 609_b undergo the second greatest blue shift (3.1 ± 0.2 nm, BFG trimer) (Figure S7 of theSupporting Information). It is also interesting to note the spread of the eigenvalue shifts for some eigenstates, indicating considerable heterogeneity and a breaking of the apparent *C*3 symmetry.

Eigenstate Delocalization *in Vacuo*. A picture of eigenstate localization/delocalization is given by the participation ratio (PPR, see Methods) and shown in Figure 3D (see also Figures S5 and S6, panel D, of theSupporting Information). A sizable degree of eigenstate delocalization is always present, although eigenstates are mainly delocalized over up to two chromophore equivalents. A maximum PPR value of 6.6 (BFG trimer) is reached. This value is less than half the number of chlorophylls per monomer so that no eigenstate is delocalized either on the entire LHCII chl array or on a single monomer. It should be noted that the PPR maximum value remains always significantly lower than the number of chlorophylls per trimer, even when calculations were performed increasing the unperturbed transition dipole strength associated with the chlorophylls and, then, the absolute values of interaction energies (not shown). However (Figure 3 and Figures S5 and S6 of the Supporting Information), a number of eigenstates are partially delocalized over the trimer, in particular those involving chl 602_a and/or 603_a, the two chla faced toward the trimer center of symmetry. These eigenstates often have the highest transition dipole strength (Figure 3 and Figures S5 and S6 of theSupporting Information). The variability of PPR among the LHCII trimers is another indication of the LHCII heterogeneity as modeled from crystal data. Moreover, PPR values clearly show that eigenstates dominated by *C*3 identified chloprophylls are not *C*3 symmetry related, another expression of symmetry breaking due to diagonal disorder.

The total interaction energy set is involved in transition dipole strength redistribution, and the presence of weak interactions, although not sufficiently intense to significantly scatter the contribution of a relevant number of chlorophylls among eigenstates (Figure 3D), is sufficient to scatter the transition dipole strength among eigenstates other than those due to the major interacting chlorophylls. This point can be envisaged by analyzing two chla couples, 611_a−612_a and 613_a−614_a, having quite extreme properties.

Chlorophylls 613_a and 614_a. These chlorophylls share a mean interaction energy of ∼71 cm^{-1} and are, structurally, the most isolated chl couples from the other pigments in the array (see the Supporting Information, Figure S1). The next most intense interactions are with 601_b (≈−14 cm^{-1}) on the same monomer and with 607_b (≈14 cm^{-1}) on an adjacent monomer (see also the Supporting Information, Figure S2). Moreover, their calculated unperturbed site energies differ by ∼330 cm^{-1}, which is much greater than their mutual interaction energy. Thus, substantially unperturbed eigenstates, representing nearly unperturbed chl site energy transitions, are, at first sight, expected. The eigenvalues (transition energies) characteristic of the eigenstates associated with the two chlorophylls substantially reflect their unperturbed site energy transitions, with values that shift in the range from 8.5 to 27 cm^{-1} (see, e.g., Figure S7 of the Supporting Information for BFG trimer). Of the nine couples of eigenstates dominated by chl 613_a or 614_a (Figure 3 and Figures S5 and S6 of the Supporting Information), and associated with the nine monomers, just five of them have eigenvectors strongly localized on the dominating chlorophylls (with the squared eigenvector contribution in the range 84−94% for 613_a and 90−93% for 614_a; the next highest chl contribution is due to the companion chl). A measure of the eigenstate localization is also obtained by the PPR values that, for the five couples of the three LHCII trimers, are in the range of 1.1−1.4 chl equivalent (Figure 3D, BFG trimer) (see also Table S1 of the Supporting Information). Two of these strongly localized eigenstates are present in the BFG trimer on monomers B and G (Figure 3 and Table S1 of the Supporting Information). This further emphasizes, among other aspects, the marked eigenstate heterogeneity on the nine monomers. However, even for these localized eigenstates, a transition dipole strength redistribution always occurs. Whereas the transition dipole strengths associated with the five 613_a dominated eigenstates are in the range of 15.9−20.9 D^2, more or less the unperturbed transition dipole strength (20.2 D^2), the transition dipole strengths associated with the five 614_a dominated eigenstates are in the range of 26.8−30.8 D^2 (see also Figure 3C and Figures S5 and S6 and Table S1 of the Supporting Information for the BFG trimer, as an example), higher than the unperturbed value. This indicates that also for eigenstates strongly dominated by a single chl contribution, the role of the

other chlorophylls of the array, although apparently marginal, cannot be excluded *a priori* and that the relative orientations play an important role (eq 8).

The remaining four couples of eigenstates, although dominated by chl 613_a and 614_a, are relatively more delocalized as also shown by the enhanced PPR values (Figure 3 and Figures S5 and S6 and Table 1 of the Supporting Information for eigenstates dominated by chl $F613_a$ and $F614_a$). Interestingly, the total transition dipole strength associated with these eigenstates is quite variable, having values in the wide range of 2.3−31 D^2 for 613_a dominated eigenstates and 15.7−37.8 D^2 for 614_a dominated eigenstates. This, besides being another indication of the great variability among the trimeric LHCII monomers, clearly indicates a broken *C*3 symmetry of the LHCII complex when eigenstates are considered (see also Table S1 of the Supporting Information as an example).

To summarize, although the chl 613_a and 614_a couples appear to be structurally isolated, they cannot be considered as being an independent (or substantially independent) excitonic dimer. In fact, in a number of cases the correlated eigenstates have their eigenvectors almost localized on a single chl, 613_a or 614_a, whereas in other cases the eigenstates dominated by chl 613_a and 614_a contain significant contributions of other different chlorophylls. Moreover, the eigenstate characteristics are strongly influenced by the unperturbed chl energy site distribution.

Chlorophylls 611_a and 612_a. This is one of the most tightly packed and strongest interacting chl couples (interaction energy mean value of ∼167 cm^{-1} for the BFG trimer), whereas the next highest mean interactions are less intense (611_a−610_a = −31 cm^{-1}; 612_a−610_a = 29 cm^{-1}, 611_a−601_b = 31 cm^{-1}, 612_a−602_a = 19 cm^{-1}; see Figure S2 of the Supporting Information). The interaction energy between 611_a and 612_a is nearly equal to the mean difference between the two calculated unperturbed site energy transitions (Figure 2) and, then, eigenstates with significant excitonic character are expected. However, only three couples 611_a−612_a, one for each trimer (G, H, and J monomers, Figure 3 and Figures S5 and S6 and Table S2 of the Supporting Information), contribute principally to two eigenstates, showing PPR values in the range of 1.8−2.3 chl equivalent. In these couples chl 611_a dominates the shorter wavelength eigenstates, which are characterized by a mean transition dipole strength of 3.8 D^2 and PPR values around two equivalent molecules (2.1−2.3). Chl 612_a dominates the longer wavelength eigenstates, characterized by mean transition dipole strength of 37.2 D^2 and PPR values in the range of 1.8−2.2. The transition dipole strength is then distributed, as a mean, in a ratio of 1/10 (shorter/longer). Even though the total mean contribution of the two chlorophylls 611_a and 612_a to each of the two eigenstates examined is ≈90% (as squared contribution to the eigenvectors), the total transition dipole strength shared by the two eigenstates is significantly different, with values of 32.5, 41.7, and 49 D^2 (40.4 D^2 is expected for an isolated dimer). This indicates that the transition dipole strength is also shared with other eigenstates. The remaining six 611_a−612_a couples contribute to more than two eigenstates, and relevant contributions by other chlorophylls are present in the eigenvectors dominated by them (Figure 3A and Figurs S5 and S6 of the Supporting Information). This further highlighs the absence of *C*3 symmetry among eigenstates of the same trimer and also emphasizes the heterogeneity among eigenstates dominated by the same site defined chlorophylls.

The two strongly interacting chlorophylls 611_a and 612_a are, along with chl 610_a, part of a chla cluster located on the stromal side (610_a−611_a−612_a cluster; see, e.g., ref 53). This chla trio has, in fact, two chlorophylls b as nearest neighbor, namely 601_b and 608_b. However, as discussed above, chl 610_a interacts weakly ($|V| \sim 30$ cm^{-1}) with both 611_a and 612_a, whereas the interaction 611_a−612_a is quite strong (∼167 cm^{-1}). Chlorophyll 610_a is located at the same distance from both chl 612_a and 608_b but interacts more strongly with chl 608_b (∼78 cm^{-1}). However, the unperturbed transition energy gap between 610_a and 608_b is 4-fold that with 612_a. Moreover, a relevant number of weak interactions with other chlorophylls of the array is also present. Although in terms of interacting energies and distances this chl trio seems to be isolated from the rest of chromophore array, the present structure-based calculation does not provide support for localized eigenstates among chl 610_a−611_a−612_a (Figure 3 and Figures S5 and S6 of the Supporting Information). Of the nine monomers analyzed, only in one case (C monomer, Supporting Information, Figure S5) do the three eigenstates associated mainly with these chlorophylls contain a relevant contribution of all the three molecules; otherwise, the total chl 611_a and 612_a squared contribution to eigenvectors dominated by 610_a is between 3 and 5% and *vice versa* (see Figure 3 and Figures S5 and S6 and Tables S2 of the Supporting Information as an example). The total transition dipole strength shared by this chla trio is quite variable and falls in the range of 39−85 D^2. Interestingly, just the C monomer chl trio shares a total of 64 D^2, nearly the expected value for three interacting chlorophylls alone. Once again, a significant variability emerges from the analysis of the nine monomers identified in the X-ray structure. Four 610_a dominated eigenstates have PPR values in the range of 1.22−1.24 chl equivalent (e.g., the B and G eigenstates, Supporting Information, Table S2), indicating strongly localized states, although the associated transition dipole strengths are in the range of 9.3−12.7 D^2 (Figure 3C and Figures S5C and S6C of the Supporting Information), considerably less than the unperturbed chla value (20.2 D^2). The remaining eigenvectors involve chl contributions other than that of chl 611_a and 612_a, resulting in higher PPR values (Figure 3C and Figures S5C and S6C of the Supporting Information). This further highlights the effect of the unperturbed energy site distribution on the eigenstate distribution (see the Supporting Information, Table S3, for an example of this effect) as well as the absence of *C*3 symmetry among chl eigenstates of the LHCII trimer.

The eigenstate variability previously described for monomers in a trimer as well as among the three trimers modeled by crystal analysis[20] suggests a role of protein conformational degrees of freedom in modulating the transition energy disorder and, in turn, the mutual interaction among chlorophylls. Distinct reversible spectroscopic states have been recently observed in LHCII single-molecule fluorescence kinetics measurement during irradiation,[99] and the role of fluctuations among different protein conformational substates in determining fluctuations of the pigment site energy transitions was discussed by these authors. The three different LHCII trimers can be assumed to represent the freezing of three different accessible protein conformations. It should be noted that small variations of the chl macrocycle deformations induce sizable chl site transition energies changes,[19] and these small variations can be induced by small changes of the protein backbone conformation during transitions among accessible

conformational tiers in its potential energy hypersurface (see, e.g., ref 100).

Calculated Absorption Spectra *in Vacuo*. Knowledge of both the unperturbed site transition energies and transition dipole strengths as well as the set of eigenvalues (transition energies) and the redistributed transition dipole strengths generated by chl interactions permits calculation of the expected absorption spectrum due to structural properties only (i.e., in the absence of medium effects). To this end, a calculated chl band shape (see Methods[19]) is associated with each transition energy. The resulting absorption spectra (1) for the unperturbed set of chl transition energies and transition dipole strengths and (2) for the eigenstates generated in the presence of chl interactions are shown in Figure 4. It can be seen that interactions among chlorophylls broadens the absorption spectrum and, interestingly, the spectroscopic separation between chlb and chla absorption regions becomes more evident, as occurs in measured absorption spectra. However, the first moments of the two bandshapes, representing the mean wavelength value weighted by the band shape distribution, are very similar, being 641 nm for the absorption spectrum in the absence of chl−chl interaction and 642 nm for that calculated using the eigenstates.

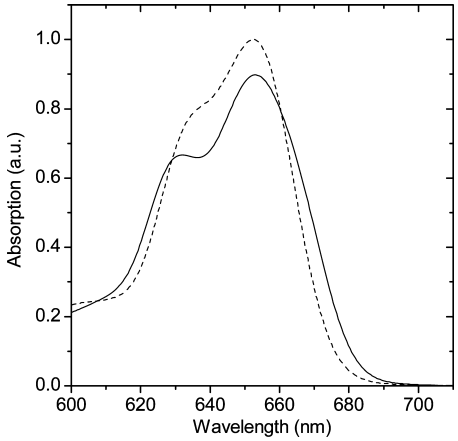

Figure 4. Calculated absorption spectra for the BFG LHCII trimer *in vacuo*. The 42 eigenstates, giving the vertical transition energies and the sub-band area (redistributed dipole strengths), calculated *in vacuo* (n = 1, D = 1) and in the presence of interactions among chlorophylls (see text) have been used to calculate the absorption spectrum (—). The chl band shape associated with each eigenstate is calculated according to the method of Zucchelli et al.[98] in terms of a modified vibronic Franck−Condon factors set that fit chla in diethyl ether and in the presence of a mean phonon mode of frequency ν = 20 cm^{-1} and coupling S = 0.8 (see Methods). As a comparison, the absorption spectrum calculated using the unperturbed chl transition energies and the respective unperturbed dipole strengths (no chl−chl interactions) is also shown (- - -). The areas of the two spectra are the same, and an inhomogeneous contribution of 155 cm^{-1} is used.

Calculation of LHCII Trimer Eigenstates in the Presence of a Medium. Figure 4 shows that the calculated LHCII absorption spectra *in vacuo* have absorption maxima at wavelengths shorter than those experimentally measured (~676 nm). As *in vacuo* it is the bare LHCII structure that is only considered, other sources of transition energy modulation need to be taken into account to match the measured spectral characteristics. In this respect we consider the intervening heterogeneous medium, represented by the protein host and the bulk solvent, in modulating the unperturbed site energy transitions and the chl−chl interactions. As already mentioned, determination of both the protein refractive index and dielectric constant is not straightforward. However, a number of suggestions to the effects of the medium can be drawn independently by the exact choice of the values of these parameters. As discussed under Theory, when the presence of a medium, described in terms of its refractive index, n, and its dielectric constant, D, is considered, a number of consequences arise. The impact of the medium on the properties of the chromophore array can be summarized as (1) a red shift of the chromophore electronic transition energies via the solvatochromic effect (eq 1), (2) an increase of the chl transition dipole strength (eq 3, $n \neq 1$), and (3) the presence of an attenuation factor $\alpha < 1$ (eqs 2 and 5). The presence of the medium then affects chl−chl interactions by way of two opposite effects. In fact, the increased chl transition dipole strength leads to an increase in chl−chl interaction energies (eqs 2 and 5), whereas the presence of the attenuation factor, which depends on the mutual chromophore distances, reduces the absolute values of the interaction energies.

The principal effects of the presence of the medium on the elements of the matrix (Hamiltonian) defining the eigenstates of an LHCII trimer will be now examined and compared with those previously discussed under vacuum conditions.

Chlorophyll Site Transition Energies and Chl−Chl Interaction Energies: Effect of the Medium. The presence of the solvatochromic effect (eq 1) shifts the unperturbed chl Q_y site transition energies toward lower energies (red shift), and this shift is a function of the refractive index of the chl surroundings. On the basis of the estimated solvent-accessible macrocycle surfaces (see Theory, Figure 1) from the entire set of chlorophylls, a minimum of two subsets, each characterized by different surroundings and refractive indices, can be distinguished. Then, less accessible chlorophylls are embedded in a host medium with an effective refractive index presumably higher than that of the other chlorophylls. The calculations of the red shifts were performed (eq 1) using a dielectric constant D = 5 and refractive index n = 1.54 for protein-embedded chlorophylls and n = 1.36, the lowest value obtained for an adsorbed protein layer,[77] for the four chlorophylls, 605$_b$, 611$_a$, 612$_a$, and 614$_a$ of each monomer in a trimer, with the greatest accessible surfaces (Theory, Figure1). The calculated red shifts for the chl site transition energies are 21.2 and 15.2 nm, for the two chl subsets, respectively.

The chl−chl interaction energies (Figure S8 of the Supporting Information) were calculated using eq 5 with the value of n_L = 1.54,[53,80] for the refractive index involved in the attenuation coefficient, and n = 1.33, the refractive index of water, for the bulk medium (see Theory). With this choice the chla and chlb transition dipole strengths are dps ≅ 28 D^2 (eq 3) and dps ≅ 19.6 D^2, respectively (see Theory). The interplay between increased chl transition dipole strength and the presence of the attenuation factor tends, under our conditions, to be dominated by the attenuation effect (see Figure S8 of the Supporting Information). The attenuation coefficient depends on mutual chl distances that are distributed with substantial C_3 symmetry (see the Supporting Information, Figure S1). Thus, the presence of the attenuation coefficient does not lead to changes in the off-diagonal disorder that in the *in vacuo* condition was determined to be low.

It is worth noting that the interaction energy between chl 601$_b$ and 609$_b$ on facing monomers remains significant also in

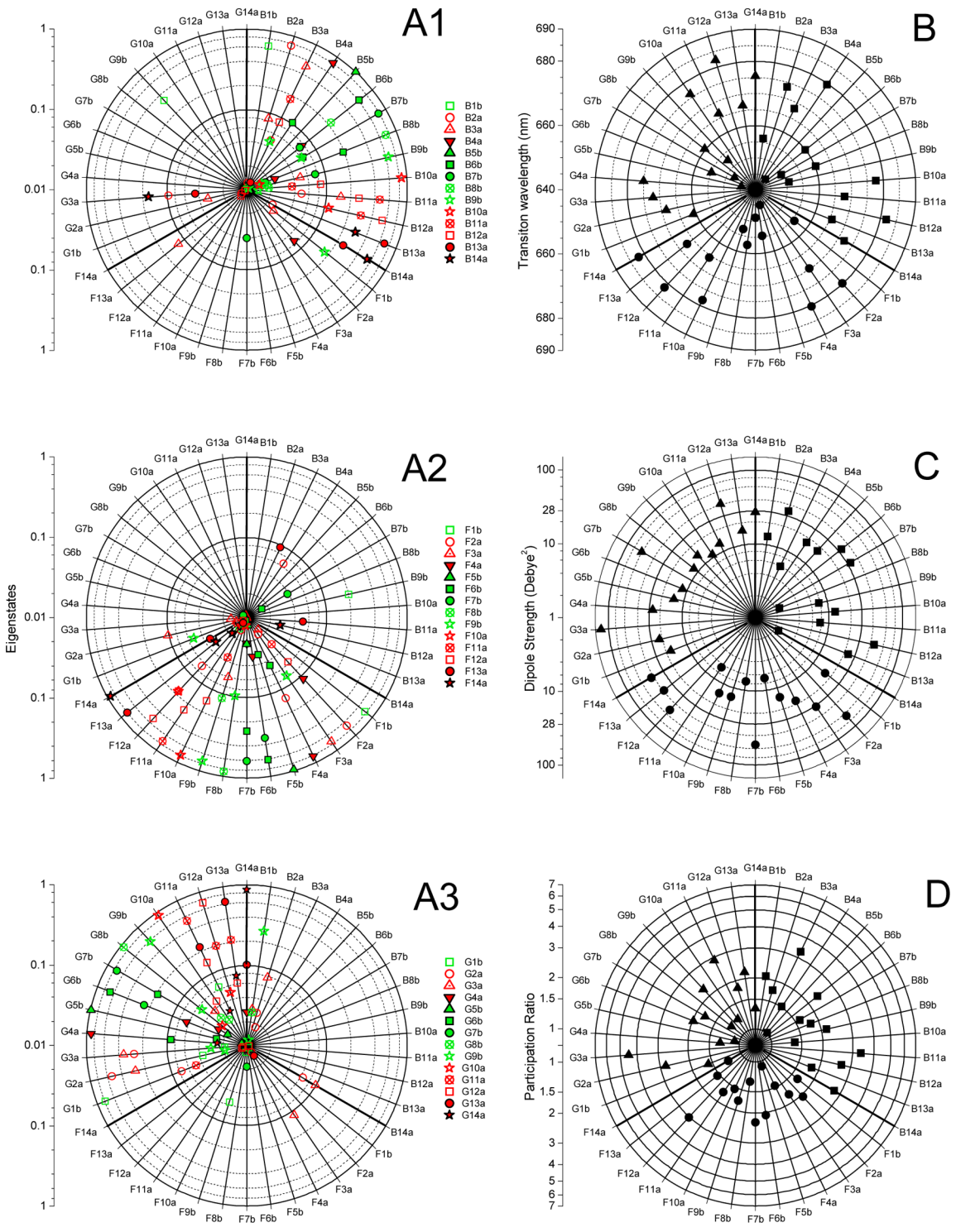

Figure 5. Eigenstate properties for the LHCII BFG trimer in the presence of the medium. Panels A1, A2, and A3 show the squared contribution of all the chlorophylls of the B, F, and G monomers, respectively, to the 42 eigenstates identified by the 42 radii and, on each radius, by the major chl contribution. The scale is logarithmic. Heavy radii mark the boundaries of monomers. (Open symbols) chlorophylls of the stromal layer; (solid symbols) chlorophylls of the lumenal layer; (red symbols) chla; (green symbols) chlb. As an example, in panel A1 the radius B1b indicates the eigenstate dominated by the contribution of chlb 601 of the B monomer. Looking to the same marked radius in the three panels, the complete chl contributions to the given eigenstate can be obtained. Panel B shows the transition wavelengths (eigenvalues) associated with the 42 eigenstates specified by the dominant chl contribution and evaluated in terms of the chl site transitions modified by the solvatochromic effect due to the presence of the medium. The entire network of chl−chl interactions is taken into account. Panel C shows the eigenstate-associated dipole strengths as redistributed by the presence of chl−chl interactions in logarithmic scale. The initially unperturbed chla site dipole strength used in this calculation is dps ≈ 28 D^2, modified by the medium. Panel C shows the inverse participation ratio associated with each eigenstate in logarithmic scale. This parameter gives a measure of the delocalization of the eigenstate in terms of chl equivalent. See Figure 3 for further information.

dx.doi.org/10.1021/bi201677q | *Biochemistry* 2012, 51, 2717−2736

the presence of a medium. At first sight, this might suggest a role for this chlb pair in excitation energy transfer among monomers in a trimer. However, when excitation energy equilibrium is attained, the excited state population located on chlb is very low. Thus, even in the presence of sizable interaction energy, their role in intertrimer energy transfer is expected to be marginal.

Eigenstates: Effect of the Medium. The numerical diagonalization of matrices of chl interaction energies and site transition energies modified by the presence of the medium (solvatochromic shift) define 42 eigenstates that, for the BFG trimer, are shown in Figure 5. Chl contributions to eigenvectors are changed with respect to vacuum condition (Figures 3 and 5A). The maximum PPR value (Figure 5D) is now 4.6 chl equivalents (DIJ trimer, not shown) compared with 6.6 chl equivalents *in vacuo*, indicating the presence of less delocalized eigenvectors. This need not have been necessarily the case as the presence of the medium attenuates the interaction energies but, at the same time, increases the chl transition dipole strength (eq 3) with respect to the vacuum case. However, as mentioned above, in the present case it is the first effect that dominates. The redistributed transition dipole strengths are shown in Figure 5C for the BFG trimer.

It is interesting to note that the presence of the medium seems to increase the eigenstate variability, either within trimers or among trimers, with respect to vacuum conditions. This renders the unequivocal grouping of eigenstates even more problematical than *in vacuo*. In the following we take several examples to illustrate and discuss these points.

Chlorophylls 613_a and 614_a: Effect of the Medium. As already shown, of the nine eigenstates dominated by chlorophylls of the lumenal couples 613_a–614_a, five of them are strongly localized *in vacuo*, with the next highest contribution due to the companion chl and with apparently negligible contributions by other chlorophylls. Two of these couples of localized eigenstates are present in the BFG trimer (Figure 3 and Table S1 of the Supporting Information). When the medium is taken into account, the picture becomes more complicated (Figure 5A) with changes that involve all eigenstates. For example (Tables S1 and S3 of the Supporting Information), the eigenvectors dominated by the lumenal chl B14a and G13a now contain contributions that are absent *in vacuo*, as also indicated by the enhanced PPR values. On the contrary, eigenstates dominated by F13a and F14a become more localized than *in vacuo* (compare PPR values, Figures 3 and 5). Furthermore, an enhanced variability of the total transition dipole strength shared by 613_a and 614_a dominated eigenstates is observed, with values of 24.8, 80.9, and 42.4 D^2 for the B, F, and G monomers, respectively, two of which are less than the 56 D^2 expected for an isolated dimer (see the Supporting Information, Table S4). *In vacuo* the total shared transition dipole strengths are, instead, higher than that expected for a dimer. In particular, the total redistributed transition dipole strength over the three chla couples 613_a–614_a of the BFG trimer is slightly greater than 8 chla equivalents *in vacuo*, whereas slightly more than 5 chla equivalents is obtained in the presence of the medium. Thus, the medium breaks down the localized eigenstates of this chl dimer as other significant chl contributions are now present.

The above-reported transition dipole strength variability may seem, at first sight, surprising. However, it should be considered that it is impossible to envisage the outcome of the transition dipole strength redistribution (eq 8) for an interacting chl array with a relatively great number of chlorophylls as in the LHCII trimer. Besides the contribution of each site to the eigenvectors ($e_{k,i}$, eq 8), the relative transition dipole moment orientations are also involved and a sizable number of small contributions can be present that lead to a total non-negligible contributions when considered together.

Chl 610_a–611_a–612_a: Effect of the Medium. When the presence of the medium is considered, the interactions among chlorophylls of this trio and their nearest neighbors become reduced (Figure S8 of the Supporting Information) with significant changes in the eigenstates of the 610_a–611_a–612_a trio (Figure 5 and Table S5 of the Supporting Information for the BFG trimer). The contribution of chl 610a to the eigenstates dominated by the other two chlorophylls is now increased, although to different extents, and *vice versa* (Supporting Information, Figure S5 and Table S5). However, eigenstates dominated by chlorophylls of the 610_a–611_a–612_a trio also contain relevant contributions by other chlorophylls (Figure 5). Thus, although this chla trio seems to be quite isolated in the chl array and, when the presence of the medium is taken into account, there are indications of an enhanced contribution of all three chlorophylls to each of the three eigenstates dominated by these chlorophylls, it is therefore perhaps simplistic to consider 610_a–611_a–612_a chlorophylls as forming an (excitonic) trimer. Furthermore, the mean transition dipole strength shared by these three chlorophylls is 71 D^2, about 15% less than the 84 D^2 expected for three independent chlorophylls. This is a clear indication of significant transition dipole strength redistribution to other chlorophylls out of chlorophyll trios and emphasizes that all interactions, albeit weak, must be considered in the eigenstates description. The importance of interactions between pigments in different monomer subunits has been emphasized by modeling the CD spectrum of ref 101.

Calculated Absorption Spectra in the Presence of the Medium. The calculated absorption spectra of the three LHCII trimers in terms of the eigenstate transition energies and the calculated values of redistributed transition dipole strengths are shown in Figure 6. Analogously to the calculation performed for the *in vacuo* conditions (Figure 4), a chl band shape, calculated using the vibronic frequencies and Franck–Condon factors[19] at room temperature, is associated with each eigenstate. The calculated eigenvalues are the 0–0 transition energies, and the band shape is weighted by the associated transition dipole strength. It can be seen (Figure 6) that, despite the approximations, the calculated spectra are quite similar to the room temperature measured absorption spectrum of isolated trimeric LHCII preparation dissolved in an aqueous buffer. The variability among the calculated absorption spectra for the three different LHCII trimers reflects their previously discussed structural variability. We emphasize that these spectra are the outcome of a direct calculation of the chl site energies in terms of structural parameters treated together with the discussed approximations and not the results of a best fit analysis that minimize free (or almost free) parameters. Each of the three absorption spectra can be envisaged as the absorption of a single LHCII trimeric complex frozen in the crystal. The variability among spectra can then be understood as a partial mapping of the overall spectroscopic variability induced by the conformational variability of the protein complex itself.[99,102] This variability should then be connected with the inhomogeneous contribution to the ensemble absorption spectrum. We stress that the use of a site inhomogeneous contribution to the

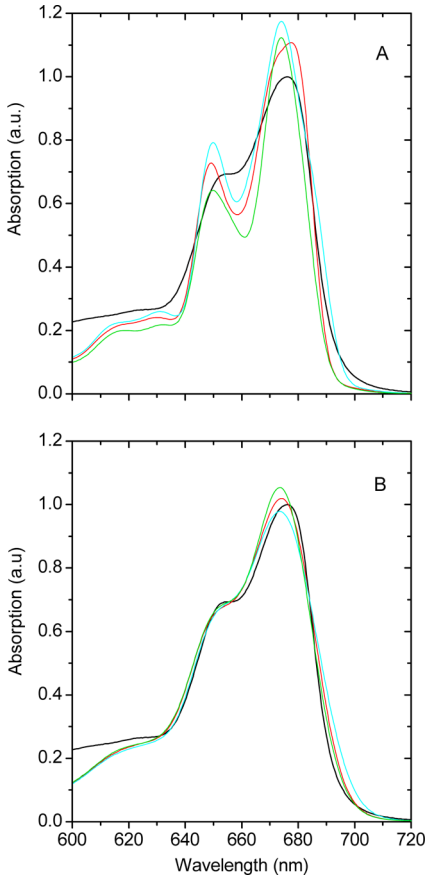

Figure 6. Calculated absorption spectra for the three LHCII trimers. (Red) BFG trimer; (cyan) CEH trimer; (green) DIJ trimer. The 300 K measured absorption spectrum of an LHCII peparation resuspended in an aqueous solution is also shown (continuous line) for comparison. The eigenstates used to calculate the spectra have been obtained with refractive index n = 1.36 for chl 605_b, 611_a, 612_a, 614_a (see text) and n = 1.54 for all other chlorophylls to evaluate the solvatochromic shifts of the site transitions. n = 1.54 is also the asymptotic refractive index used to evaluate chl−chl interaction energies. The chl band shape associated with each calculated eigenstate has been estimated according to the method of Zucchelli et al.,[98] using the modified vibronic pattern that fit chla in solution and in the presence of a mean phonon mode of frequency ν = 20 cm^{-1} and coupling S = 0.8. Panel A shows the inhomogeneous contribution to the chl band shape of 55 cm^{-1} and panel B the inhomogeneous contribution of 155 cm^{-1}.

calculated absorption spectrum of each trimer should be considered as an approximation used to roughly simulate the optical response of the ensemble sample to permit comparison with the experimental measured spectrum. Two different inhomogeneous contributions to the absorption spectra are shown in Figure 6.

It is interesting to note that the overall distribution and intensities of the optical transitions in the Q_y region analyzed here do not display particularly marked differences in the presence or absence of chl−chl interactions (Figure 4) (see, however, Figure S7 of the Supporting Information, where the eigenstate wavelength transitions are directly compared with the corresponding unperturbed transition wavelength). This means that, from a biological point of view, the antenna light-harvesting properties of this important antenna complex are not expected to be particularly influenced by these interactions. The result that, in a leaf, the main light-harvesting occurs in the chl region near 650 nm with the long wavelength chla tail not extended significantly above 705 nm[103] seems to be, basically, a consequence of the chl site energy distribution and not the result of the chl−chl interactions.

It should be emphasized that although the entire set of chl−chl interactions gives rise to eigenstates that have the majority of their transition wavelengths shifted by < ±2 nm (see, e.g., Figures S7 of the Supporting Infomration), nevertheless the eigenvectors contain the contribution of a number of different chlorophylls. This is also shown by the PPR values (Figures 3 and 5), interpreted as chl equivalents of an eigenstate. These delocalized eigenstates are expected to give rise to CD signals greater than the chl intrinsic one, which, of course, is what is experimentally observed, in general terms.[104] We recall that both Q_y−Q_x and Q_x−Q_x interactions as well as interaction among chl electronic transitions and carotenoids have not been taken into account in the present calculations. It cannot be excluded that a closer match between the measured and calculated absorption spectra could be obtained by conderidering the whole set of interactions. In particular, it has been shown[101] that these intreractions play a role in the description of the LHCII CD spectrum in the entire spectral range. Yet, the purpose of the present study is that of proving a reasonable description of the measured optical spectra with a minimal number of variables and to examine the variability of individual LHCII trimers, based on the limited coordinate sets avalaible from crystallographic studies.

The calculated LHCII absorption spectra (Figure 6) contain a number of sub-bands due to the presence of red eigenstates that define 0−0 absorption transition at wavelengths longer than 680 nm (see, e.g., Figure 5B). The low-temperature emission spectrum[105] of the LHCII crystal is strongly red-shifted with respect to the same protein complex frozen in a solvent, and the fluorescence decay is shortened. In a number of papers it is suggested that the LHCII crystal conformation described by Liu at al.[20] is a particular conformation, indicated as a quenched conformation, involved in NPQ.[105−107] This has been contested by Kühlbrandt and co-workers,[108] defending the point of view that both the red emission and the shortened fluorescence decay lifetime are due to sample self-absorption and the crystal structure of LHCII is that of an unquenched complex. To date, it is not completely clear if the properties of the chl−protein complex are modified by the different crystallization procedures. It is well-known that the spectroscopic characteristics of LHCII (see, e.g., refs 40, 44, 51, 52, 101, 102 and 109−115), and in particular the fluorescence yield (see, e.g., refs 112 and 116−118), are sensitive to environmental conditions. It is also worth noting that the structural models of LHCII resolved by Liu et al.[20] and Barros et al.[108] were obtained from crystals packed in different symmetry groups. Then it is not unlikely that crystal packing could also influence the spectroscopic properties of this chl−protein complex, as suggested by the recent investigation of van Oort et al.[107]

The sets of eigenstates used to calculate the absorption spectra of the three trimers have been also used to calculate the linear dichroism spectra. The results are shown in Figure S9 of the Supporting Information.

Comparison with Other Approaches. In a previous paper Novoderezkhin et al.[53] estimated the eigenstate electronic transitions by a numerical fit of the LHCII optical spectra using 14 unperturbed site energies as free fit parameters. Muh et al.[57] presented 14 eigenstate energies obtained by quantum mechanics/molecular mechanics calcu-

lations based on one of the three trimer structures analyzed by Liu et al.[20] Moreover, in recent papers Fleming and co-workers[56,66] present a first direct indication of an aqueous dissolved trimeric LHCII energy landscape analyzing the quantum coherence in 2D-visible spectroscopy. Common to these papers is the assignment of 14 different eigenstates (absorption transitions). However, as discussed above, the presence of diagonal disorder, of structural origin, leads to a symmetry breaking and 42 different eigenstates are, in principle, present in a trimer. In other words, the *C*3 site related chlorophylls contribute differently to the various eigenstates (see, e.g., Table 4) and, then, no strictly *C*3 related eigenstates are present. Thus, to compare the 42 eigenstates of each trimer calculated in this study (Figure 5) with the previous results, it is necessary to group them into reduced subsets of 14 eigentates. The simplest, although rough, choice is to consider the eigenstates dominated by *C*3 site related chlorophylls as the same eigenstate, ignoring the presence of different chl contributions to the eigenvectors, and to evaluate a sort of "mean" eigenvalue set, each with its spread value. This can be done when a dominant site contribution to the various eigenvectors is clearly identified or, in other words, the eigenstates are delocalized over a limited number of chlorophylls, as is the case in our calculations (Figure 5). The reduced 14 calculated "mean" site transition energies are shown in Figure 7A as a frequency-ordered sequence that is substantially linear. Comparison with the frequency-ordered sequence of the chl transition energies given by Calhoun et al.[66] shows that the calculated "mean" site transition energies are all shifted toward lower energies. This shift is about 50−60 cm^{-1}, as evaluated by the linear fit of the two ordered sequences (data not shown). The choice of the medium refractive indices that characterize the protein chl environment in a protein medium, and determine the solvatochromic shift, is an open problem and, as previously discussed, is rather arbitrary. The data in Figure 7A are calculated using n = 1.54, and a better match (Figure 7B) between the frequency-ordered sequences can be obtained by lowering the bulk protein refractive index to n = 1.45, whereas n = 1.36 is maintained for those chlorophylls with the higher solvent-accessible surface (see Theory). In this case, however, the calculated absorption spectra become all shifted toward shorter wavelengths (Figure 7C), giving a worse match with the measured LHCII spectrum. A similar spectral mismatch is also reported by Schlau-Cohen et al.[56] In Figure 7B the eigevalues (transition energies) of the eigenstates given by Novoderezkin et al.[53] and Muh et al.[57] are also shown as frequency-ordered sequences. We observe differences for the values calculated by Muh et al.[57] at the two energy extremes, but these differences are decreased when their estimated uncertainties (∼100 cm^{-1}) are taken into account.

It is interesting to compare the different eigenstates obtained by the different approches putting into correlation their transition wavelengths (eigenvalues) and the dominating chl contribution to the respective eigenvectors (Figure 8). The identification of the dominant contribution can be, however, ambiguous when the eigenvectors contain relevant contribution by different chl sites. This is the case for the eigenvectors reported by Novoderezkin et al.,[53] as indicated by their higher PPR values with respect to those obtained in this paper (not shown), and a clear-cut indication of the dominating chl site is, for a number of cases, problematical. When this occurs, multiple wavelength transitions have been assigned to the dominant site in Figure 8. Moreover, their assignment

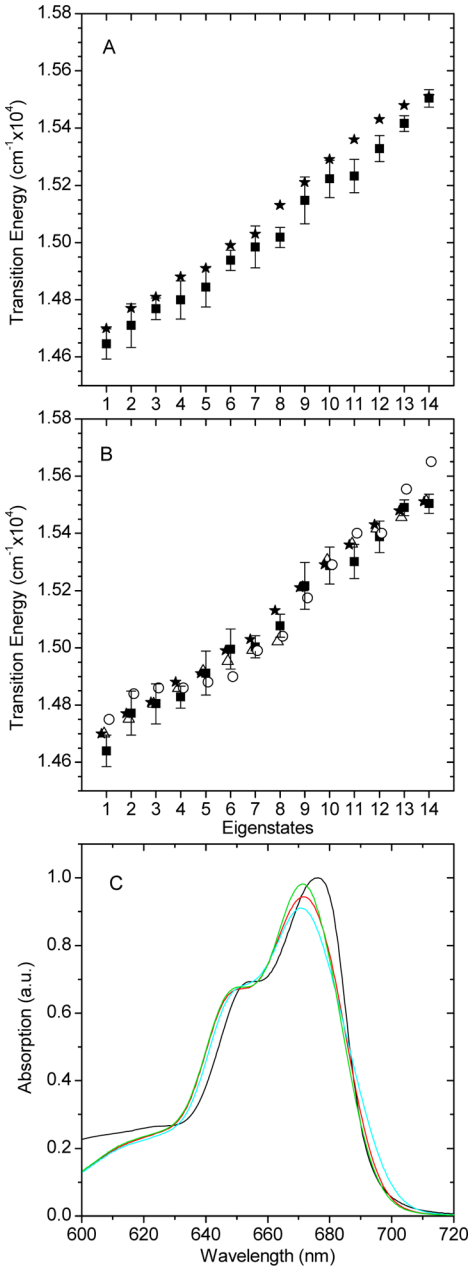

Figure 7. Mean transition frequencies for the reduced set of 14 eigenstates. (A) Frequency ordered transition energies associated with the calculated eigenstates (■) using refractive index n = 1.33 for chl dipole strength estimation (chla dps ≈ 28 D^2), n = 1.36 for the site transition energies solvatochromic shift of the most accessible chlorophylls (Figure 1) and n = 1.54 for the others chlorophylls. This last refractive index is also used to evaluate the asymptotic attenuation factor in the interaction energies calculations. These parameters are the same as used to calculate the absorption spectra shown in Figure 6. The eigenvalues calculated for the three LHCII trimers are mediated by grouping them in terms of the 14 main chl contributions (see text). (★) The 14 transitions are as proposed by Calhoun et al.[66] (B) The same as (A) (■) but with the solvatochromic shift calculated with refractive index n = 1.45 for the buried chlorophylls, whereas n = 1.36 is maintained to calculate the solvatochromic shifts of the most accessible chlorophylls. The refractive index n = 1.45 determines also the asymptotic attenuation factor in the interaction energies calculation. The 14 transitions obtained by numerical best fit analysis[53] (△) and by structural quantum chemical analysis[57] (○) are also shown. (C) The absorption spectra for the three different LHCII trimers when calculated in terms

dx.doi.org/10.1021/bi201677q | *Biochemistry* 2012, 51, 2717−2736

Figure 7. continued

of the eigenstates obtained using the same parameters as in panel B. (Red) BFG trimer; (cyan) CEH trimer; (green) DIJ trimer. The RT absorption spectrum measured for a LHCII preparation resuspended in an aqueous buffer is shown for comparison (—).

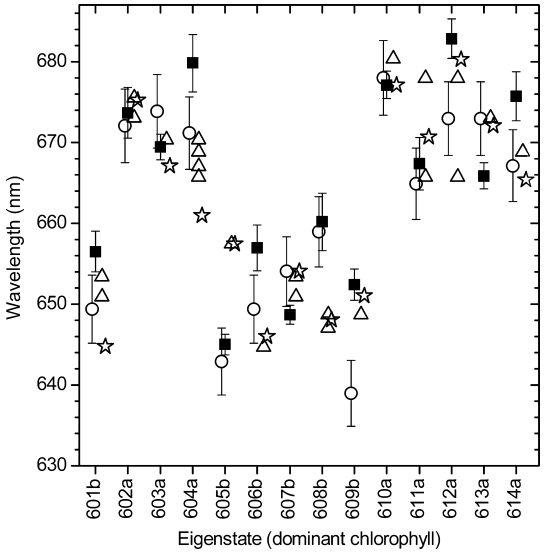

Figure 8. Transition wavelengths (eigenvalues) as a function of the LHCII eigenstates. Eigenstates are identified by the dominant chl contribution. (■) Eigenstate transition wavelengths were calculated using, as starting data, the unperturbed site transition energies obtained by normal-mode analysis of chl ring structural deformations (see also Theory). These values have been obtained with refractive indexes n = 1.54 for the embedded chlorophylls and n = 1.36 for the other chlorophylls (see Theory) to represent the medium envelope. The mean values among the 9 calculated eigenstates for each dominating chl site are shown with their spread. (○) Fourteen eigenstate wavelengths were calculated by Muh et al.[57] along with their suggested distribution widths; (△) 14 eigenstates obtained by the numerical fits analysis of LHCII spectra by Novoderezkin et al.;[53] (☆) 14 exciton energies determined from 2D optical spectroscopies by Calhoun et al.[66] The dominat chl contributions to these last eigenstates have been obtained using the Hamiltonian published by Schlau-Cohen et al.[56] (see the text).

represents a choice among the results of a great number of different realizations of the disorder and, as the authors frankly admit, other eigenstate descriptions cannot be excluded. It should also be noted that the best fit of the optical linear spectra chosen by Novoderezkin et al.[53] to describe the experimental data is obtained using 16 D^2 as value of the effective transition dipole strength (i.e., dps/n^2). This choice, however, manifests itself in changes of the value of the refractive index that, on the basis of eq 3,[89,90] yields a medium refractive index n = 1.31, less than that of water. This further emphasizes the problem connected with the description of the chl surroundings in a chl−protein complex. The exciton energies determined from 2D electronic spectroscopies by Calhoun et al.[66] are also shown in Figure 8. In this case, to identify the dominant chl contribution associated with these exciton frequencies, we have calculated the 14 eigenstates in terms of the Hamiltonian published by Schlau-Cohen et al.,[56] where the interaction energies calculated by Frahmcke and Walla[54] are used. Some discrepancies in the assignment of the eigenstates occur. The lowest energy eigenstate is, in our calculation, dominated by chl 612_a, as is also suggested by Schlau-Cohen et al.,[56] whereas the other approaches suggest chl 610_a as the dominating chl contribution. However, Muh et al.[57] suggest that this finding is valid at low temperature and, on the basis of a LHCII site-directed mutagenesis analysis,[59] propose a temperature-dependent red shift of the eigenstate dominated by chl 612_a. It is interesting to note that using chl site binding mutational analysis of LHCII and CP29 and analyzing absorption and emission spectra at room temperature, Remelli et al.[58] considered chl 612_a as the redmost chl form. The effect of temperature on the LHCII absorption spectrum is a problem that has been studied in the past, and several possible explanations have been proposed,[22,28,119,120] but no clear-cut rationalization has yet been obtained. In terms of structure-based calculations we also find that the transition energy of the 613_a-dominated eigenstate is higher than that of the 614_a-dominated eigenstate, the opposite obtained by the other approaches (Figure 8). Our calculation suggests that eigenstates dominated by chl 608_b are the reddest chlb eigenstates. This is the same assignment given by Muh et al.,[57] whereas both Novoderezhkin et al.[53] and Calhoun et al.[66] propose a higher energy transition. Also, we found that the eigenstate dominated by chl 605_b is at higher frequencies than that assigned by Calhoun et al.[66] and Novoderezhkin et al.[53] and is in accordance with the assignment of Muh et al.[57] This overall picture is maintained when eigenstates calculated with n = 1.45 are considered (not shown).

Site Chlorophyll Energy Transitions. As previously discussed, knowledge of the unperturbed energy transitions, characteristic of each chl site, is essential for the comprehension of different properties of chl−protein complexes. These chl site energies, calculated here in terms of the chl macrocycle deformations[19] as obtained from the LHCII crystal data analysis, are compared with those obtained by other approaches[53,56,57] (Figure 9). In particular, Muh et al.,[57] using combined quantum mechanics/molecular mechanics approaches, calculated 14 chl site energies on the basis of structural LHCII data, whereas Novoderezhkin et al.[53] and Schlau-Cohen et al.[56] indirectly estimated the site energies by fitting analyses. The results obtained by the two different approaches based on structural data show quite a good correlation. The major differences are for chl 606_b, 609_b, and 612_a. We emphasize that each transition wavelength is, in this case, characteristic of a chl molecule in its environment and is not the eigenvalue of an eigenstate dominated by the same chl. The two approaches based on structural data indicate chl 605_b as the most blue-shifted chlb and chl 608_b as the reddest chlb, in contrast to the assigned site transitions fitted by both Novoderezkin et al.[53] and Schlau-Cohen et al.[56] We emphasize, however, that an estimation of the site energy spread is not provided in these last two cases. Chl 608_b as the redmost chlb was already suggested,[19] a property that is maintained when both medium effects and chl−chl interaction, giving rise to the eigenstates, are taken into account, as previously discussed (Figure 8). It is also interesting that chl 604_a site transition is, as also obtained by Muh et al.,[57] at a lower energy than that assigned by the two numerical approaches.[53,56] The redmost site transition energy is, according to our approach and as a mean, associated with chl 612_a, in agreement with mutational analysis,[58] whereas the other approaches suggest chl 610_a as the redmost site.

It should be noted that most attempts to use the crystallographic structure to explain aspects of LHCII antenna

dx.doi.org/10.1021/bi201677q | *Biochemistry* 2012, 51, 2717−2736

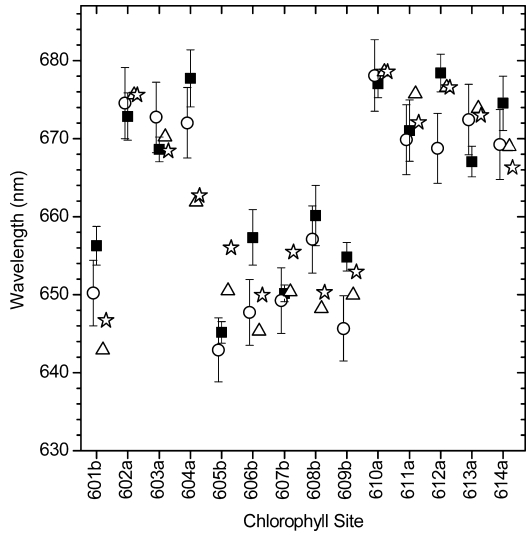

Figure 9. Chlorophyll site unperturbed transition wavelengths. (■) Site transition wavelengths were calculated using normal-mode analysis of chl ring deformations as obtained by crystallographic LHCII description.[20] These values are also the result of the action of the solvatochromic shift calculated using $n = 1.54$ for the embedded chlorophylls (see Theory) and $n = 1.36$ for the other chlorophylls. The wavelength transitions for sites identified by the same chl have been mediated, and the distribution spreads are shown as error bars. (○) Chl site energies were calculated according to the method of Muh et al.[57] with their suggested distribution. The site transition wavelengths indirectly determined in terms of parameter minimization of LHCII spectra numerical fits by Novoderezkin et al.[53] (△) and Schlau-Cohen et al.[56] (☆) are also shown. Both of these data have been shifted toward lower energies by 300 cm^{-1} as the published data do not contain reorganization energies.

function are based on the study of a single monomer or trimer. In the present study a large eigenstate variability among monomers of the same trimer and among trimers is demonstrated, which should be considered.

■ CONCLUSIONS

The LHCII chl data, modeled by the analysis of the LHCII crystal,[20] have been used to directly evaluate the intrinsic chl site transitions as modulated by the environment, in terms of chl macrocycle deformations. These site transitions, calculated for all of the chlorophylls in the three LHCII trimers analyzed using the crystallographic data,[20] have been used, with the calculated interaction energies in the ideal dipole approximation, to evaluate the complete set of eigenstates for each of the three LHCII trimers in the absence (*in vacuo*) and in the presence of a medium. Despite a number of approximations and considering the intrinsic errors of the structural input data, the calculated absorption spectra for the three LHCII trimers in terms of calculated eigenstates and their redistributed transition dipole strength show a quite good correspondence with the measured absorption spectrum of a LHCII preparation resuspended in a buffer. This can be taken as an indication that the approach used here is substantially robust, and a number of conclusions relating to microscopic parameters can be drawn:

(1) The sets of chl−chl distance, evaluated among the calculated chl four nitrogens centers, for the three monomers in each of the three LHCII trimers are, at this level of precision, largely equivalent, and they are also equivalent among the three monomers. The small off-diagonal disorder leads to nearly equivalent sets of interaction energies. Thus, the LHCII chl array shows, in terms of both chl−chl distances and interaction energies, a substantial C3 symmetry.

(2) The differences of chl macrocycle deformations in the same monomeric chl binding site of a trimer have a marked influence on the set of chl unperturbed site transition energies (Figure 2). They show marked variations among monomers of the same trimer, leading to a C3 symmetry breaking in LHCII. The origin of these deformations is probably due to fluctuations of the protein backbone structure inside its complex conformational energy potential that induce strain of the chl macrocycle. Then, in terms of unperturbed chl transition energies, the diagonal disorder leads to a breakdown of the LHCII C3 symmetric structure.

(3) The absence of C3 symmetry for the unperturbed site transition energies results in the absence of C3 symmetry in the LHCII trimer eigenstates induced by the presence of mutual interactions among chromophores. The eigenvectors dominated by chlorophylls identified in terms of the same monomer site contain differently distributed contributions of other chlorophylls in the array. Both the redistributed transition dipole strengths, due to chromophore interaction, and the participation ratio are also not C3 symmetry related.

(4) The light-harvesting antenna properties of LHCII are not particularly influenced by the presence of chl−chl interactions but are mainly the results of the unperturbed chl site energy distribution.

■ ASSOCIATED CONTENT

Ⓢ Supporting Information

Solvent screening of electronic couplings as a function of refractive index. Chlorophyll mutual distances representation for the BFG trimer of LHCII. Absolute values of the *in vacuo* interaction energies among chlorophyll of the three trimers BFG, CEH, and DIJ. Eigenstate properties of the two trimers CEH and DIJ *in vacuo*. Transition wavelength differences due to chlorophyll interactions for the BFG trimer. Absolute values of the interaction energies among chlorophyll of the BFG trimer in the presence of the medium. Calculated linear dichroism spectra in the presence of the medium. Parameters of eigenstates dominated by chl 613_a and 614_a of the BFG trimer in the absence and in the presence of the medium. Parameters of the eigenstates dominated by chl 610_a, 611_a, and 612_a of the BFG trimer in the absence and in the presence of the medium. Effect of modifying a chlorophyll unperturbed site transition energy on the LHCII trimer eigenstates. This material is available free of charge via the Internet at http://pubs.acs.org.

■ AUTHOR INFORMATION

Corresponding Author

*Phone: +390250314775. Fax: +390250314815. E-mail: giuseppe.zucchelli@unimi.it.

Notes

The authors declare no competing financial interest.

■ ABBREVIATIONS USED

Chl, chlorophyll; dps, transition dipole strength; LHCII, light harvesting complex II; PPR, participatio ratio

REFERENCES

(1) van Grondelle, R., Dekker, J. P., Gillbro, T., and Sundstrom, V. (1994) Energy transfer and trapping in photosynthesis. *Biochim. Biophys. Acta 1187*, 1−65.

(2) Green, B. R., and Durnford, D. G. (1996) The chlorophyll-carotenoid proteins of oxigenic photosynthesis. *Annu. Rev. Plant Physiol. Plant Mol. Biol. 47*, 685−714.

(3) Jennings, R. C., Bassi, R., and Zucchelli, G. (1996) Antenna structure and energy transfer in higher plant photosystems, in *Topics in Current Chemistry. Electron Transfer II* (Mattay, J., Ed.), pp 147−181, Springer-Verlag, Berlin, Germany.

(4) Hankamer, B., Barber, J., and Boekema, E. J. (1997) Structure and membrane organization of photosystem II in green plants. *Annu. Rev. Plant Physiol. Plant Mol. Biol. 48*, 641−671.

(5) Boekema, E. J., van Breemen, J. F. L., van Roon, H., and Dekker, J. P. (2000) Arrangement of photosystem II supercomplexes in crystalline macrodomains within the thylakoid membrane of green plant chloroplasts. *J. Mol. Biol. 301*, 1123−1133.

(6) Renge, I., and Avarmaa, R. (1985) Specific solvation of chlorophyll a: solvent nucleophility, hydrogen bonding and steric effects on absorption spectra. *Photochem. Photobiol. 42*, 253−260.

(7) Gudowska-Nowak, E., Newton, M. D., and Fajer, J. (1990) Conformational and environmental effects on bacteriochlorophyll optical spectra: correlations of calculated spectra with structural results. *J. Phys. Chem. 94*, 5795−5801.

(8) Giuffra, E., Zucchelli, G., Sandona, D., Croce, R., Cugini, D., Garlaschi, F. M., Bassi, R., and Jennings, R. C. (1997) Analysis of some optical properties of native and reconstituted photosystem II antenna complex, CP29: pigment binding sites can be occupied by chlorophyll a or chlorophyll b and determine the spectral forms. *Biochemisty 36*, 12984−12993.

(9) Rogl, H., and Kühlbrandt, W. (1999) Mutant trimers of light-harvesting complex II exhibit altered pigment content and spectroscopic features. *Biochemistry 42*, 16214−16222.

(10) van Amerongen, H., Valkunas, L., and van Grondelle, R. (2000) *Photosynthetic Excitons*, World Scientific, Singapore.

(11) Nishigaki, A., Ohshima, S., Nakayama, K., Okada, M., and Nagashima, U. (2001) Application of molecular orbital calculations to interpret the chlorophyll spectral forms in pea photosystem II. *Photochem. Photobiol. 73*, 245−248.

(12) French, C. S., Brown, J. S., and Lawrence, M. C. (1972) Four universal forms of chlorophyll a. *Plant Physiol. 49*, 421−429.

(13) Zucchelli, G., Jennings, R. C., and Garlaschi, F. M. (1990) The presence of the long-wavelength chlorophyll a spectral forms in the light-harvesting chlorophyll a/b protein complex II, J. *Photochem. Photobiol. B−Biol. 6*, 381−394.

(14) Zucchelli, G., Dainese, P., Jennings, R. C., Breton, J., Garlaschi, F. M., and Bassi, R. (1994) Gaussian decomposition of absorption and linear dichroism spectra of outer antenna complexes of photosystem II. *Biochemistry 33*, 8982−8990.

(15) Hemerijk, P. W., Kwa, S. L. S., van Grondelle, R., and Dekker, J. P. (1992) Spectroscopic properties of LHCII, the main ligth-harvesting chlorophyll-a/b protein complex from chloroplast membranes. *Biochim. Biophys. Acta 1098*, 159−166.

(16) Krawczyk, S., Krupa, Z., and Maksymiec, W. (1993) Stark spectra of chlorophylls and carotenoids in antenna pigment-proteins LHCII and CPII. *Biochim. Biophys. Acta 1143*, 273−281.

(17) Nussberger, S., Dekke, J. P., Kuhlbrandt, W., van Bolhuis, B. M., van Grondelle, R., and van Amerongen, H. (1994) Spectroscopic characterization of 3 different monomeric forms of the main chlorophyll a/b binding-protein from chloroplast membranes. *Biochemistry 33*, 14775−14783.

(18) Schubert, A., Leupold, D., Beenken, W., Ehlert, J., Hoffmann, P., and Lokstein, H. (1997) Direct observation of spectral substructure in the Q(y)-absorption band of light harvesting complex II by nonlinear polarisation spectroscopy in the frequency domain at low temperature. *Biochim. Biophys. Acta 1321*, 195−199.

(19) Zucchelli, G., Brogioli, D., Casazza, A. P., Garlaschi, F. M., and Jennings, R. C. (2007) Chlorophyll ring deformations modulates Q_y electronic energies in chlorophyll-protein complexes and generates spectral forms. *Biophys. J. 93*, 2240−2254.

(20) Liu, Z., Yan, H., Wang, K., Kuang, T., Zhang, J., Gui, L., An, X., and Chang, W. (2004) Crystal structure of spinach major light-harvesting complex at 2.72 Å resolution. *Nature 428*, 287−292.

(21) Jennings, R. C., Bassi, R., Garlaschi, F. M., Dainese, P., and Zucchelli, G. (1993) Distribution of the chlorophyll spectral forms in the chlorophyll-protein complexes of photosystem II antenna. *Biochemistry 32*, 3203−3210.

(22) Zucchelli, G., Garlaschi, F. M., and Jennings, R. C. (1996) Thermal broadening analysis of the light harvesting complex II absorption spectrum. *Biochemistry 35*, 16247−16254.

(23) Litvin, F. F., and Sineshchekov, V. A. (1965) Molecular organisation of chlorophyll and energetics of the initial stages of photosynthesis, in *Bioenergetics of Photosynthesis* (Govindjee, Ed.), pp 619−661, Academic Press, New York.

(24) Gillie, J. K., Small, G. J., and Golbeck, J. H. (1989) Nonphotochemical hole burning of the native antenna complex of photosystem I (PSI200). *J. Phys. Chem. 93*, 1620−1627.

(25) Tang, D., Jankowiak, R., Seibert, M., Yocum, C. F., and Small, G. J. (1990) Excited-state structure and energy-transfer dynamics of two different preparations of the reaction center of photosystem II: a hole-burning study. *J. Phys. Chem. 94*, 6519−6522.

(26) Reddy, R. N. S., Lyle, P. A., and Small, G. J. (1992) Applications of spectral hole burning spectroscopies to antenna and reaction center complexes. *Photosynth. Res. 31*, 167−193.

(27) Kwa, S. L. S., Völker, S., Tilly, N. T., van Grondelle, R., and Dekker, J. P. (1994) Polarized site-selection spectroscopy of chlorophyll a in detergent. *Photochem. Photobiol. 59*, 219−228.

(28) Peterman, E. J. G., Pullerits, T., van Grondelle, R., and van Amerongen, H. (1997) Electron−phonon coupling and vibronic fine structure of light harvesting complex II of green plants: temperature dependent absorption and high-resolution fluorescence spectroscopy. *J. Phys. Chem. 101*, 4448−4457.

(29) Sandonà, D., Croce, R., Pagano, A., Crimi, M., and Bassi, R. (1998) Higher plants light harvesting proteins. Structure and function as revealed by mutation analysis of either protein or chromophore moieties. *Biochim. Biophys. Acta 1365*, 207−214.

(30) Pieper, J., Voigt, J., and Small, G. J. (1999) Clorophyll a Franck-Condon factors and excitation energy transfer. *J. Phys. Chem. B 103*, 2319−2322.

(31) Pieper, J., Irrgang, K.-D., Rätsep, M., Voigt, J., Renger, G., and Small, G. J. (2000) Assignment of the lowest Qy-state and spectral dynamics of the CP29 chlorophyll a/b antenna complex of green plants: a hole-burning study. *Photochem. Photobiol. 71*, 574−581.

(32) Rätsep, M., Johnson, T. W., Chitnis, P. R., and Small, G. J. (2000) The red-absorbing chlorophylla antenna states of photosystem I: a holeburning study of *Synechocystis* sp. PCC 6803 and its mutants. *J. Phys. Chem. 104*, 836−847.

(33) Pieper, J., Rätsep, M., Irrgang, K.-D., and Freiberg, A. (2009) Chromophore-chromophore and chromophore-protein interactions in monomeric light-harvesting complex II of green plants studied by spectral hole burning and fluorescence line narrowing. *J. Phys. Chem. 113*, 10870−10880.

(34) Reppert, M., Naibo, V., and Jankowiak, R. (2010) Accurate modeling of fluorescence line narrowing difference spectra: direct measurement of the single-site fluorescence spectrum. *J. Chem. Phys. 133*, 014506.

(35) Pieper, J., Ratsep, M., Trostmann, I., Paulsen, H., Renger, G., and Freiberg, A. (2011) Excitonic energy level structure and pigment-protein interactions in the recombinant water-soluble chlorophyll protein. I. Difference fluorescence line-narrowing source. *J. Phys. Chem. B 115*, 4042−4052.

(36) Pieper, J., Ratsep, M., Trostmann, I., Schmitt, F. J., Theiss, C., Paulsen, H., Eichler, H. J., Freiberg, A., and Renger, G. (2011) Excitonic energy level structure and pigment-protein interactions in the recombinant water-soluble chlorophyll protein. II. Spectral hole-burning experiments. *J. Phys. Chem. B 115*, 4053−4065.

(37) Jankowiak, R., Reppert, M., Zazubovich, V., Pieper, J., and Reinot, T. (2011) Site selective and single complex laser-based spectroscopies: a window on excited state electronic structure, excitation energy transfer, and electron−phonon coupling of selected photosynthetic complexes. *Chem. Rev. 111*, 4546−4598.
(38) Lokstein, H., Leupold, D., Voigt, B., Nowak, F., Ehlert, J., Hoffmann, P., and Garab, G. (1995) Nonlinear polarization spectroscopy in the frequency domain of light-harvesting complex II: absorption band substructure and exciton dynamics. *Biophys. J. 69*, 1536−1543.
(39) Peterman, E. J. G., Dekker, F. M., van Grondelle, R., and van Amerongen, H. (1995) Chlorophyll a and carotenoid triplet states in light-harvesting complex II of higher plants. *Biophys. J. 69*, 2670−2678.
(40) Ruban, A. V., Dekker, J. P., Horton, P., and van Grondelle, R. (1995) Temperature dependence of chlorophyll fluorescence from the light harvesting complex II of higher plants. *Photochem. Photobiol. 61*, 216−221.
(41) Ruban, A. V., Calkoen, F., Kwa, S. L. S., van Grondelle, R., Horton, P., and Dekker, J. P. (1997) Characterisation of the aggregated state of the light harvesting complex of photosystem II by linear and circular dichroism spectroscopy. *Biochim. Biophys. Acta 1321*, 61−70.
(42) Barzda, V., Istokovics, A., Simidjiev, I., and Garab, G. (1996) Structural flexibility of chiral macroaggregates of light-harvesting chlorophyll a/b pigment-protein complexes. Light-induced reversible structural changes associated with energy dissipation. *Biochemistry 35*, 8981−8985.
(43) Connelly, J. P., Müller, M. G., Gatzen, G., Mullineaux, C. W., Ruban, A. V., Horton, P., and Holzwarth, A. R. (1997) Ultrafast spectroscopy of trimeric light harvesting complex II from higher plants. *J. Phys. Chem., B 101*, 1902−1909.
(44) Barzda, V., Peterman, E. J. G., van Grondelle, R., and van Amerongen, H. (1998) The influence of aggregation on triplet formation in light-harvesting chlorophyll a/b pigment-protein complex II of green plants. *Bochemistry 37*, 546−551.
(45) Naqvi, K. R., Javorfi, T., Melo, T. B., and Garab, G. (1999) More on the catalysis of internal conversion in chlorophyll a by an adjacent carotenoid in light-harvesting complex (Chla/b LHCII) of higher plants: time-resolved triplet-minus-singlet spectra of detergent-perturbed complexes. *Spectrochim. Acta, Part A 55*, 193−204.
(46) Croce, R., Müller, M. G., Bassi, R., and Holzwarth, A. R. (2001) Carotenoid-to-chlorophyll energy transfer in recombinant major light-harvesting complex (LHCII) of higher plants. I. Femtosecond transient absorption measurements. *Biophys. J. 80*, 901−915.
(47) Formaggio, E., Cinque, G., and Bassi, R. (2001) Functional architecture of the major light-harvesting complex from higher plants. *J. Mol. Biol. 314*, 1157−1166.
(48) Gradinaru, C. C., van Grondelle, R., and van Amerongen, H. (2003) Selective interaction between xanthophylls and chlorophylls in LHCII probed by femtosecond transient absorption spectroscopy. *J. Phys. Chem. B 107*, 3938−3943.
(49) Caffarri, S., Croce, R., Cattivelli, L., and Bassi, R. (2004) A look within LHCII: differential analysis of the Lhcb1-3 complexes building the major trimeric antenna complex of higher-plant photosynthesis. *Biochemistry 43*, 9467−9476.
(50) Palacios, M. A., Caffarri, S., Bassi, R., van Grondelle, R., and van Amerongen, H. (2004) Stark effect measurements on monomers and trimers of reconstituted light-harvesting complex II of plants. *Biochim. Biophys. Acta 1656*, 177−188.
(51) van Oort, B., van Hoek, A., Ruban, A. V., and van Amerongen, H. (2007) Aggregation of light-harvesting complex II leads to formation of efficient excitation energy traps in monomeric and trimeric complexes. *FEBS Lett. 581*, 3528−3532.
(52) van Oort, B., van Hoek, A., Ruban, A. V., and van Amerongen, H. (2007) Equilibrium between quenched and nonquenched conformations of the major plant light-harvesting complex studied with high-pressure time-resolved fluorescence. *J. Phys. Chem. B 111*, 7631−7637.
(53) Novoderezhkin, V. I., Palacios, M. A., van Amerongen, H., and van Grondelle, R. (2005) Excitation dynamics in the LHCII complex of higher plants: modeling based on the 2.72 Å crystal structure. *J. Phys. Chem. B 109*, 10493−10504.
(54) Frähmcke, J. S., and Walla, P. J. (2006) Coulombic couplings between pigments in the major light-harvesting complex LHC II calculated by transition density cube method. *Chem. Phys. Lett. 430*, 397−403.
(55) Duffy, C. D., Ruban, A. V., and Barford, W. (2008) Theoretical investigation of the role of strongly coupled chlorophyll dimers in photoprotection of LHCII. *J. Phys. Chem. B 112*, 12508−12515.
(56) Schlau-Cohen, G. S., Calhoun, T. R., Ginsberg, N. S., Read, E. L., Ballottari, M., Bassi, R., van Grondelle, R., and Fleming, G. R. (2009) Pathways of energy flow in LHCII from two-dimensional electronic spectroscopy. *J. Phys. Chem. B 113*, 15352−15363.
(57) Müh, F., Madjet, M. El-A., and Renger, T. (2010) Structure-based identification of energy sinks in plant light-harvesting complex II. *J. Phys. Chem. B 114*, 13517−13535.
(58) Remelli, R., Varotto, C., Sandonà, D., Croce, R., and Bassi, R. (1999) Chlorophyll binding to monomeric light-harvesting complex − a mutation analysis of chromophore-binding residues. *J. Biol. Chem. 274*, 33510−33521.
(59) Rogl, H., Schödel, R., Lokstein, H., Kühlbrandt, W., and Schubert, A. (2002) Assignment of spectral substructures to pigment-binding sites in higher plant light-harvesting complex LHC-II. *Biochemistry 41*, 2281−2287.
(60) Belgio, E., Casazza, A. P., Zucchelli, G., Garlaschi, F. M., and Jennings, R. C. (2010) Band shape heterogeneity of the low-energy chlorophylls of CP29: absence of mixed binding sites and excitonic interactions. *Biochemistry 49*, 882−892.
(61) Hamm, P., Lim, M., and Hochstrasser, R. M. (1998) Structure of the amide I band of peptides measured by femtosecond non-linear infrared spectroscopy. *J. Phys. Chem. 102*, 6123−6138.
(62) Asplund, M. C., Zanni, M. T., and Hochstrasser, R. M. (2000) Two-dimensional infrared spectroscopy of peptides by phase-controlled femtosecond vibrational photon echoes. *Proc. Natl. Acad. Sci. U.S.A. 97*, 8219−8224.
(63) Mukamel, S. (2000) Multidimensional femtosecond correlation spectroscopies of electronic and vibrational excitations. *Annu. Rev. Phys. Chem. 51*, 691−729.
(64) Zanni, M. T., and Hochstrasser, R. M. (2011) Two-dimensional infrared spectroscopy: a promising new method for the time resolution of structures. *Curr. Opin. Struct. Biol. 11*, 516−522.
(65) Brixner, T., Stenger, J., Vaswani, H. M., Cho, M., Blankenship, R. E., and Fleming, G. R. (2005) Two-dimensional spectroscopy of electronic couplings in photosynthesis. *Nature 434*, 625−628.
(66) Calhoun, T., Ginsberg, N. S., Schlau-Cohen, G. S., Cheng, Y.-C., Ballottari, M., Bassi, R., and Fleming, G. R. (2009) Quantum coherence enabled determination of the energy landscape in light-harvesting complex II. *J. Phys. Chem. B 113*, 16291−16295.
(67) Kühlbrandt, W., Wang, D. N., and Fujiyoshi, Y. (1994) Atomic model of plant light-harvesting complex by electron crystallography. *Nature 367*, 614−621.
(68) Standfuss, R., van Scheltinga, A. C. T., Lamborghini, M., and Kuhlbrandt, W. (2005) Mechanisms of photoprotection and non-photochemical quenching in pea light-harvesting complex at 2.5A resolution. *EMBO J. 24*, 919−928.
(69) Jentzen, W., Simpson, M. C., Hobbs, J. D., Song, X., Ema, T., Nelson, N. Y., Medforth, C. J., Smith, K. M., Veyrat, M., Mazzanti, M., Ramasseul, R., Marchon, J.-C., Taleuchi, T., Goddart, W. A. III, and Shelnutt, J. A. (1995) Ruffling in a series of nichel(II) meso-tetrasubstituted porphyrins as a model for the conserved ruffling of the EME of cytochromes c. *J. Am. Chem. Soc. 117*, 11085−11097.
(70) Jentzen, W., Song, X.-Z., and Shelnutt, J. (1997) Structural characterization of synthetic and protein bound porphyrins in terms of the lowest frequency normal coordinates of the macrocycle. *J. Phys. Chem. 101*, 1684−1699.

(71) Shelnutt, J. A., Song, X.-Z., Ma, J.-G., Jia, S.-L., Jentzen, W., and Medford, C. J. (1998) Nonplanar porphyrins and their significance in protein. *Chem. Soc. Rev. 27*, 31−41.
(72) Sobolev, V., Sorokine, A., Prilusky, J., Aola, E. E., and Edelman, M. (1999) Automated analysis of interatomic contacts in protein. *Bioinformatics 15*, 327−332.
(73) Frauenfelder, H., Wolynes, P. G., and Austin, R. H. (1999) Biological physics. *Rev. Mod. Phys. 71*, S419−S430.
(74) Bakhshiev, N. G. (1961) Universal molecular interactions and their effect on the position of the electronic spectra of molecules in two component solutions 1: theory (liquid solutions). *Opt. Spectrosc. 10*, 717−726.
(75) Krawczyk, S. (1989) The effects of hydrogen bonding and coordination interaction in visible absorption and vibrational spectra of chlorophyll a. *Biochim. Biophys. Acta 976*, 140−149.
(76) Seely, G. R., and Jensen, R. G. (1965) Effect of solvent on the spectrum of chlorophyll. *Spectrochim. Acta 21*, 1835−1845.
(77) Vörös, J. (2004) The density and refractive index of adsorbing protein layers. *Biophys. J. 87*, 553−561.
(78) Paillotin, G., Leibl, W., Gapiński, J., Breton, J., and Dobek, A. (1998) Light gradients in spherical photosynthetic vesicles. *Biophys. J. 75*, 124−133.
(79) Kleima, F. J., Hofmann, E., Gobets, B., van Stokkum, I. H. M., van Grondelle, R., Diederichs, K., and van Amerongen, H. (2000) Förster excitation energy transfer in peridinin-chlorophyll-a protein. *Biophys. J. 78*, 344−353.
(80) Gruszecki, W. I., Grudzinski, W., Banaszek-Glos, A., Matula, M., Kremer, P., Krupa, Z., and Sielewiesiuk, J. (1999) Xantophyll pigments in light-harvesting complex II monomolecular layers: localization, energy transfer and orientation. *Biochim. Biophys. Acta 1412*, 173−183.
(81) Renge, I. R., van Grondelle, R., and Dekker, J. P. (1996) Matrix and temperature effects on the absorption spectra of β-carotene and pheophytin a in solution and in green plant photosystem II. *J. Photochem. Photobiol. Chem. 96*, 109−121.
(82) Takashima, S., and Schwan, H. P. (1965) Dielectric dispersion of crystalline powders of amino acids, peptides and proteins. *J. Phys. Chem. 69*, 4176−4182.
(83) Varma, S., and Jakobsson, E. (2004) Ionization states of residues in Ompf and mutants: effects of dielectric constant and interactions between residues. *Biophys. J. 86*, 690−704.
(84) Schutz, C. N., and Warshel, A. (2001) What are the dielectric "constants" of proteins and how to validate electrostatic models? *Proteins: Struct., Funct., Genet. 44*, 400−417.
(85) Still, W. C., Tempczyka, A., Hawley, R. C., and Hendrickson, T. (1990) Semianalytical treatment of solvation for molecular mechanics and dynamics. *J. Am. Chem. Soc. 112*, 6127−6129.
(86) Fiedor, L., Kania, A., Mysliwa-Kurdziel, B., Orzel, L., and Stochel, G. (2008) Understanding chlorophylls: central magnesium ion and phytyl as structural determinants. *Biochim. Biophys. Acta (Bioenerg.) 1777*, 1491−1500.
(87) Fiedor, L., Stasiek, M., Mysliwa-Kurdziel, B., and Strzalka, K. (2003) Phytol as one of the determinants of chlororphyll interactionsin solution. *Photosynth. Res. 78*, 47−57.
(88) Linnanto, J., Martiskainen, J., Lehtovuori, V., and Ihalainen, J. (2006) Excitation energy transfer in the LHC-II trimer: a model based on the new 2.71 Å structure. *Photosynth. Res. 87*, 267−279.
(89) Knox, R. S. (2003) Dipole and oscillator strengths of chromophores in solution. *Photochem. Photobiol. 77*, 492−496.
(90) Knox, R. S., and Spring, B. Q. (2003) Dipole strengths in the chlorophylls. *Photochem. Photobiol. 77*, 497−501.
(91) Palacios, M. A., de Weerd, F. L., Ihalainen, J. A., van Grondelle, R., and van Amerongen, H. (2002) Superradiance and exciton (de)localisation in light harvesting complex II from green plants? *J. Phys. Chem. B 106*, 5782−5787.
(92) Knox, R. S., and van Amerongen, H. (2002) Refractive index dependence of the Förster excitation energy transfer rate. *J. Phys. Chem. B 106*, 5289−5293.
(93) Curutchet, C., Scholes, G. D., Mennucci, B., and Cammi, R. (2007) How solvent control electronic energy transfer and light harvesting: toward a quantum-mechanical description of reaction field and screening effects. *J. Phys. Chem. B 111*, 13253−13265.
(94) Scholes, G. D., Curutchet, C., Mennucci, B., Cammi, R., and Tomasi, J. (2007) How solvent controls electronic energy transfer and light harvesting. *J. Phys. Chem. B 111*, 6978−6982.
(95) Sauer, K., Lindsay Smith, J. R., and Schultz, A. J. (1966) The dimerization of chlorophyll a, chlorophyll b and bacteriochlorphyll in solution. *J. Am. Chem. Soc. 88*, 2681−2688.
(96) Bell, R. J., and Dean, P. (1970) Atomic vibrations in vitreous silica. *Discuss. Faraday Soc. 50*, 55−61.
(97) Briggs, J. S., and Herzenberg, A. (1970) Sum rules for the vibronic spectra of helical polymers. *J. Phys. B: At. Mol. Phys. 3*, 1663−1676.
(98) Zucchelli, G., Jennings, R. C., Garlaschi, F. M., Cinque, G., Bassi, R., and Cremonesi, O. (2002) The calculated in vitro and in vivo chlorophyll a absorption bandshape. *Biophys. J. 82*, 378−390.
(99) Krüger, T. P. J., Novoderezhkin, V. I., Ilioaia, C., and van Grondelle, R. (2010) Fluorescence spectral dynamics of single LHCII trimers. *Biophys. J. 98*, 3093−3101.
(100) Hofmann, C., Aartsma, T. J., Michel, H., and Köhler, J. (2003) Direct observation of tiers in the energy landscape of a chromoprotein: a single molecule study. *Proc. Natl. Acad. Sci. U.S.A. 100*, 15534−15538.
(101) Georgakopoulou, S., van der Zwan, G., Bassi, R., van Grondelle, R., van Amerongen, H., and Croce, R. (2007) Understanding the changes in the circular dichroism of light harvesting complex II upon varying its pigment composition and organization. *Biochemistry 46*, 4745−4754.
(102) Krüger, T. P. J, Ilioaia, C., and van Grondelle, R. (2011) Fluorescence intermittency from the main plant light-harvesting complex: resolving shifts between intensity levels. *J. Phys. Chem. B 115*, 5071−5082.
(103) Rivadossi, A., Zucchelli, G., Garlaschi, F. M., and Jennings, R. C. (2004) Light absorption by the chlorophyll a-b complexes of photosystem II in a leaf with special reference to LHCII. *Photochem. Photobiol. 80*, 492−498.
(104) Garab, G., and van Amerongen, H. (2009) Linear dichroism and circular dichroism in photosynthesis research. *Photosynth. Res. 101*, 135−146.
(105) Pascal, A. A., Liu, Z., Broess, K., van Oort, B., van Amerongen, H., Wang, C., Horton, P., Robert, B., Chang, W., and Ruban, A. (2005) Molecular basis of photoprotection and control of photosynthetic light-harvesting. *Nature 436*, 134−137.
(106) Ruban, A. V., Berera, R., Ilioaia, C., van Stokkum, I. H., Kennis, J. T., Pascal, A. A., van Amerongen, H., Robert, B., Horton, P., and van Grondelle, R. (2007) Identification of a mechanism of photoprotective energy dissipation in higher plants. *Nature 450*, 575−578.
(107) van Oort, B., Maréchal, A., Ruban, A. V., Robert, B., Pascal, A. A., de Ruijter, N. C., van Grondelle, R., and van Amerongen, H. (2011) Different crystal morphologies lead to slightly different conformations of light-harvesting complex II as monitored by variations of the intrinsic fluorescence lifetime. *Phys. Chem. Chem. Phys. 13*, 12614−12622.
(108) Barros, T., Royant, A., Standfuss, J., Dreuw, A., and Kühlbrandt, W. (2009) Crystal structure of plant light-harvesting complex shows the active, energy-transmitting state. *EMBO. J. 28*, 298−306.
(109) Jennings, R. C., Garlaschi, F. M., and Zucchelli, G. (1991) Light-induced fluorescence quenching in the light-harvesting chlorophyll a/b protein complex. *Photosynth. Res. 27*, 57−64.
(110) Barzda, V., Jennings, R. C., Zucchelli, G., and Garab, G. (1999) Kinetic analysis of the light-induced fluorescence quenching in light-harvesting chlorophyll a/b pigment−protein complex of photosystem II. *Photochem. Photobiol. 70*, 751−759.
(111) Ruban, A. V., Pascal, A. A., Robert, B., and Horton, P. (2001) Configuration and dynamics of xanthophylls in light-harvesting antennae of higher plants. Spectroscopic analysis of isolated light-harvesting complex of photosystem II and thylakoid membranes. *J. Biol. Chem. 276*, 24862−24870.

(112) Moya, I., Silvestri, M., Vallon, O., Cinque, G., and Bassi, R. (2001) Time resolved fluorescence analysis of the photosystem II antenna proteins in detergent micelles and liposomes. *Biochemistry 40*, 12552−12561.
(113) Lampoura, S. S., Barzda, V., Owen, G. M., Hoff, A. J., and van Amerongen, H. (2002) Aggregation of LHCII leads to a redistribution of the triplets over the central xanthophylls in LHCII. *Biochemistry 41*, 9139−9144.
(114) Wentworth, M., Ruban, A. V., and Horton, P. (2003) Thermodynamic investigation into the mechanism of the chlorophyll fluorescence quenching in isolated photosystem II light-harvesting complexes. *J. Biol. Chem. 278*, 21845−21850.
(115) Santabarbara, S., Horton, P., and Ruban, A. V. (2009) Comparison of the thermodynamic landscapes of unfolding and formation of the energy dissipative state in the isolated light harvesting complex II. *Biophys. J. 97*, 1188−11897.
(116) Yan, H., Zhang, P., Wang, C., Liu, Z., and Chang, W. (2007) Two lutein molecules in LHCII have different conformations and functions: insights into the molecular mechanism of thermal dissipation in plants. *Biochem. Biophys. Res. Commun. 355*, 457−463.
(117) Ahn, T. K., Avenson, T. J., Ballottari, M., Cheng, Y.-C., Niyogi, K. K., Bassi, R., and Fleming, G. R. (2008) Architecture of a charge-transfer state regulating light harvesting in a plant antenna protein. *Science 320*, 794−797.
(118) Johnson, M. P., and Ruban, A. V. (2009) Photoprotective energy dissipation in higher plants involves alteration of the excited state energy of the emitting chlorophyll(s) in the light harvesting antenna II (LHCII). *J. Biol. Chem. 284*, 23592−23601.
(119) Renger, T., and May, V. (2000) Simulation of frequency-domain spectra: Structure-function relationships in photosynthetic pigment-protein complexes. *Phys. Rev. Lett. 84*, 5228−5231.
(120) van Amerongen, H., and van Grondelle, R. (2001) Understanding the energy transfer function of LHCII, the major light-harvesting complex of green plants. *J. Phys. Chem. B 105*, 604−617.